State of Oregon
Oregon Department of Geology and Mineral Industries
Brad Avy, State Geologist

OPEN FILE REPORT O-16-07

MONITORING THE RESPONSE AND EFFICACY OF A DYNAMIC REVETMENT CONSTRUCTED ADJACENT TO THE COLUMBIA RIVER SOUTH JETTY, CLATSOP COUNTY, OREGON

by Jonathan C. Allan and Laura L. Gabel
Oregon Department of Geology and Mineral Industries, Coastal Field Office, P.O. Box 1033, Newport, OR 97365

2016

DISCLAIMER

Cover photograph: Oblique aerial photo looking south over the Columbia River south jetty dynamic revetment project study area, Clatsop County, Oregon. The structure is located at the apex of the embayment that separates the sand beach from the vegetation line. Photograph taken by D. Best, March 09, 2015.

Oregon Department of Geology and Mineral Industries Open-File Report O-16-07
Published in conformance with ORS 516.030

For additional information:
Administrative Offices
800 NE Oregon Street, Suite 965
Portland, OR 97232
Telephone (971) 673-1555
Fax (971) 673-1562
http://www.oregongeology.org
http://www.oregon.gov/dogami

TABLE OF CONTENTS

LIST OF FIGURES

LIST OF TABLES

1.0 INTRODUCTION

The objective of this study is to document the morphological response of a dynamic revetment (also known as "gravel berm") constructed adjacent to the Columbia River south jetty, Clatsop Spit, Oregon (**Figure 1**). The structure was commissioned by the U.S. Army Corps of Engineers (USACE) in 2013 to address ongoing erosion problems along approximately 335 m (1,100 ft) of the primary foredune located adjacent to the south jetty root (**Figure 2**).

Of particular concern was the potential for a spit breach through the remaining foredune and potentially into Trestle Bay (**Figure 1**), a scenario that could have significant ramifications for the stability of the spit tip and lower Columbia River estuary. Construction of the Columbia River south jetty dynamic revetment was initiated in August 2013 and was completed in October 2013. Here we describe the results from a beach profile monitoring program initiated to document the response of the dynamic revetment, beach, and adjacent natural foredune to the effects of coastal processes, chiefly wave runup coupled with varying tide levels.

Figure 1. Location map of (A) the lower Columbia River estuary, Clatsop Plains, and jetties, (B) the much larger Columbia River littoral cell and (C) the dynamic revetment study area.

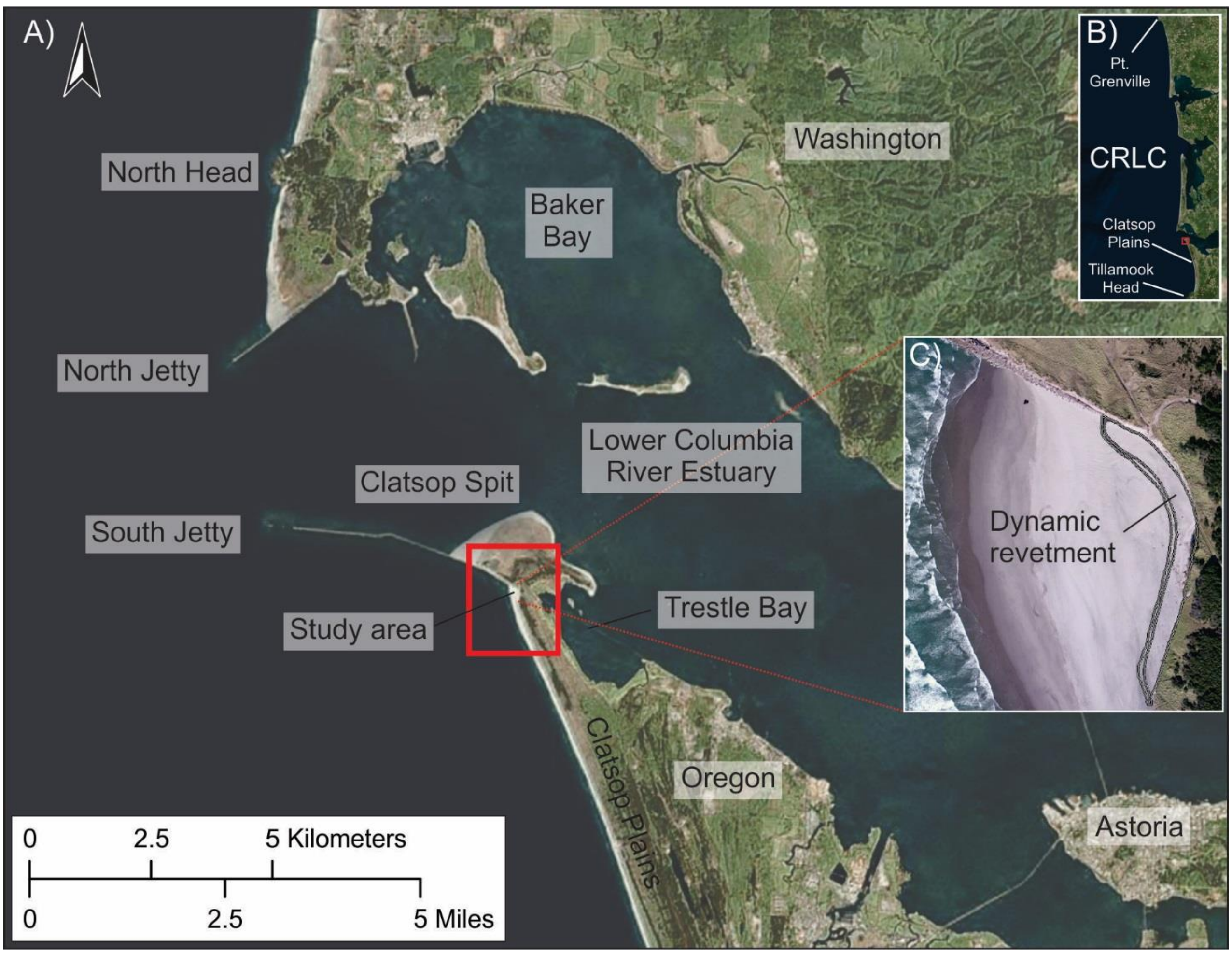

Figure 2. The jetty root (left side of photo) and the impending breach of the remaining foredune due to combinations of high wave runup coupled with high tides. Note the exposure of riprap boulders out on the beach, which have likely originated from the south jetty, as well as the collapse of the railway trestle onto the jetty riprap. View is to the south east, while an aerial perspective of the site is shown on the frontispiece and in Figure 1. (photo: J. C. Allan, DOGAMI, 2010).

2.0 STUDY OBJECTIVES

To better understand the storm-induced, seasonal, and interannual responses of the dynamic revetment adjacent to the Columbia River south jetty to the wave climate offshore the Clatsop Plains, potential negative effects of the structure on adjacent shoreline areas, and the future maintenance needs of the structure, the USACE commissioned the Oregon Department of Geology and Mineral Industries (DOGAMI), to establish a beach and shoreline monitoring system along the study area. The specific objectives of this study are to:

1. Establish a beach profile monitoring network consisting of ~30 transects and at least four survey benchmark monuments that bound the study area. The beach profile transects are to be spaced ~25 m apart along the dynamic revetment and adjacent control area, increasing to ~50-m spacing south of the immediate control area;
2. Supplement beach profile surveys of the structure with 3D topographical surveys of the dynamic revetment area achieved by using a GPS mounted on a four-wheel-drive work vehicle;
3. Undertake surveys of the area prior to commencement of the project to establish initial boundary conditions, and immediately after construction of the gravel beach. Additional surveys are to be undertaken on approximately a monthly basis during the first (2013-2014) winter season. Following the first winter, additional repeat surveys are to be undertaken on a seasonal basis, typically late summer (~September), fall (December), winter (March), and spring (June). Additional surveys may be carried out on an as-needed basis (e.g., after major storms). In all surveys, relevant terrain or feature break-lines are to be identified in the survey; these include dune crest, dune scarp, dune toe, dune-gravel intersection point, revetment crest-slope transition, gravel toe-beach intersection point, and beach terrain to mean lower low water (MLLW);
4. Make available online via the NANOOS Beach and Shoreline Changes portal (http://nvs.nanoos.org/BeachMapping) the results from the profile surveys;
5. Obtain uncontrolled aerial photography of the study area at a scale suitable for tracking the position of shoreline indicators (e.g., mean high higher water (MHHW) drift line, dune scarp-vegetation edge, revetment configuration, etc.). The photography should cover the entire project area, extending inland (east) from the foredune for 1,000 ft (305 m) offshore (west) for 2,000 ft (610 m) southward for a minimum of 5,000 ft (1,524 m), and north of the south jetty by 300 ft (91 m). The photography will be undertaken twice annually (late winter and late summer) during the first two years after project construction, and annually (late summer) thereafter for up to six years after construction. DOGAMI will endeavor to collect aerial photography within approximately two weeks of topographic beach surveys if at all possible; and,
6. Produce a report summarizing the results of the first two years of monitoring.

Results from repeat monitoring of the beach profile sites have enabled comparisons between the initial structure condition and the site's evolution. Such findings help inform the USACE and stakeholders of the following important characteristics:

1. Project performance within its first three to six years of life cycle;
2. Need for project maintenance to replace (or to relocate) material that has been displaced from the dynamic revetment; and,
3. Need for corrective action if the adjacent shore areas are experiencing negative effects associated with the project.

3.0 METHODOLOGY

3.1 Topographic Beach Mapping

3.1.1 Background

Beach profiles oriented perpendicular to the shoreline can be surveyed using a variety of approaches, including a graduated rod and chain, surveying level and staff, Total Station theodolite and reflective prism, light detection and ranging (lidar) airborne altimetry, and real-time kinematic differential global positioning system (RTK-DGPS) technology. Traditional techniques such as leveling instruments and Total Stations are capable of providing accurate representations of the morphology of a beach, but they are demanding in terms of time and effort. At the other end of the spectrum, high-resolution topographic surveys of the beach derived from lidar are ideal for capturing the three-dimensional (3D) state of the beach over an extended length of coast within a matter of hours; other forms of lidar technology are now being used to measure nearshore bathymetry out to moderate depths but are dependent on water clarity. However, lidar technology remains expensive and is impractical along small segments of shore; more importantly, the high cost effectively limits the temporal resolution of the surveys and hence the ability of the end-user to understand short-term changes in beach morphology (Bernstein and others, 2003).

Within this range of technologies, the application of RTK-DGPS for surveying the morphology of both the subaerial and subaqueous portions of the beach has become the accepted standard (Morton and others, 1993; Ruggiero and Voigt, 2000; Bernstein and others, 2003; Ruggiero and others, 2005) and is the surveying technique used in this study. The GPS is a worldwide radio-navigation system formed from a constellation of 24 satellites and their ground stations and was originally developed by the U.S. Department of Defense; in 2007 the Russian government made their GLONASS satellite network available, thereby increasing the number of satellites in the GPS to ~46 (as of February 2011). In its simplest form, GPS can be thought of as triangulation with the GPS satellites acting as reference points, enabling users to calculate their position to within several meters (e.g., using inexpensive off-the-shelf hand-held units); survey-grade GPS units are capable of providing positional and elevation measurements that are accurate to a centimeter. At least four satellites are needed mathematically to determine an exact position, although more satellites are generally available. The process is complicated because all GPS receivers are subject to error, which can significantly degrade the accuracy of the derived position. These errors include the GPS satellite orbit and clock drift plus signal delays caused by the atmosphere and ionosphere and multipath effects (where the signals bounce off features and create a poor signal). For example, hand-held autonomous receivers have positional accuracies that are typically less than about 10 m (< ~30 ft), but can be improved to less than 5 m (< ~15 ft) by using the Wide Area Augmentation System (WAAS). This latter system is basically a form of differential correction that accounts for the above errors, which is then broadcast through one of two geostationary satellites to WAAS-enabled GPS receivers.

Greater survey accuracies are achieved with differential GPS (DGPS) by using two or more GPS receivers to simultaneously track the same satellites, enabling comparisons to be made between two sets of observations. One receiver is typically located over a known reference point, and the position of an unknown point is determined relative to that reference point. With the more sophisticated 24-channel dual-frequency RTK-DGPS receivers, positional accuracies can be improved to the subcentimeter level when operating in static mode and to within a few centimeters when in RTK mode (i.e., as the rover GPS is moved about). In this study we used Trimble® 24-channel dual-frequency R7/R8 GPS receivers. This system consists of a GPS base station (R7), Zephyr Geodetic™ antenna (model 2), HPB450 radio modem, and R8 “rover” GPS (**Figure 3**).

Trimble reports that R7/R8 GPS systems have horizontal errors of approximately ±1 cm + 1 ppm (parts per million × the baseline length) and ±2 cm in the vertical (Trimble, 2005).

Figure 3. The Trimble R7 base station antenna in operation on the Clatsop Plains. Corrected GPS position and elevation information is then transmitted by an HPB450 Pacific Crest radio to the R8 GPS rover unit.

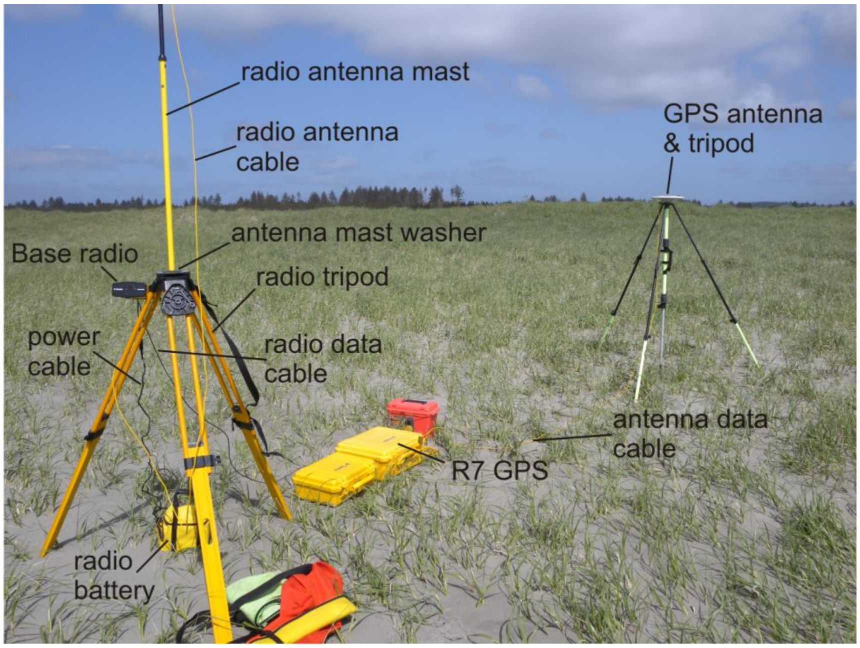

Converting a space-based positioning system to a ground-based local grid coordinate system requires a precise mathematical transformation. Although some adjustments are accomplished by specifying the map projection, datum, and geoid model prior to commencing a field survey, an additional transformation is necessary whereby the GPS measurements are tied to known ground control points (**Figure 4**). This latter step is called a GPS site calibration, such that the GPS measurements are calibrated to ground control points with known vertical and horizontal coordinates by using a rigorous least-squares adjustment procedure. Calibration is initially undertaken in the field with the Trimble TSC2 GPS controller and then re-evaluated in the office with Trimble Business Office software (version 3).

Figure 4. A 180-epoch calibration check is performed on a survey monument (Mag_nail_3). This procedure is important for bringing the survey into a local coordinate system and for reducing errors associated with the GPS survey (photo: J. C. Allan, DOGAMI).

3.1.2 Columbia River Dynamic Revetment Survey Control

Survey control near the Columbia River south jetty project area was provided by occupying several benchmarks established by the USACE (**Table 1, Figure 5**). Coordinates assigned to the benchmarks were derived by occupying a Trimble R8 GPS receiver over the established benchmark, which then receives real-time kinematic corrections via the Oregon Real Time GPS Network (ORGN, http://www.theorgn.net/). The ORGN is a network of permanently installed, continuously operating GPS reference stations established and maintained by ODOT and partners (essentially a CORS network similar to those operated and maintained by the National Geodetic Survey [NGS]) that provide real-time kinematic (RTK) correctors to field GPS users over the internet via cellular phone networks. As a result, GPS users properly equipped—such as with the Trimble system used in this study—to take advantage of these correctors can survey in the field to the 1-cm horizontal accuracy level in real time. Each benchmark was observed on at least three occasions, at different times of the day, quality control was performed and, if readings were reasonable, the readings were averaged to define the benchmark's coordinates. In all cases the Oregon State Plane coordinate system, northern zone (meters) was used, while the vertical datum was relative to the North American Vertical Datum of 1988 (NAVD88). **Table 2** shows the relative variability identified when comparing the mean derived benchmark coordinate and the original ORGN/OPUS derivations presented in **Table 1**. As can be seen in **Table 2**, differences in the horizontal and vertical values at the various benchmarks were typically less than 2 cm (i.e., within one standard deviation [σ]).

Table 1. Survey benchmarks used to calibrate GPS surveys of the Columbia River dynamic revetment. BASE identifies the location where the GPS base station was established during each respective survey.

Benchmark Name	Northing (m)	Easting (m)	Elevation (m)
KA(BASE)	2229445.841	290022.768	8.413
IR_RPC_4	2229096.740	290447.800	3.307
IR_RPC_6	2229398.459	289846.015	7.141
Mag_nail_1	2229811.087	289531.734	5.241
Mag_nail_2	2229667.316	289874.709	5.321
Mag_nail_3	2229543.142	290176.123	5.392

Notes: Coordinates are expressed in the Oregon State Plane coordinate system, northern zone (meters) and the vertical datum is the North American Vertical Datum of 1988 (NAVD88). Control provided using both horizontal and vertical values derived by averaging multiple separate GPS occupations with survey control provide by the Oregon Reference Geodetic Network (ORGN).

Figure 5. The Columbia River dynamic revetment beach profile monitoring network established adjacent to the south jetty. Note: the Eastjetty transect (red line) is a long-term monitoring site established in 1997 (http://www.oregongeology.org/nanoos/data/img/lg/EastJetty_EDA.png).

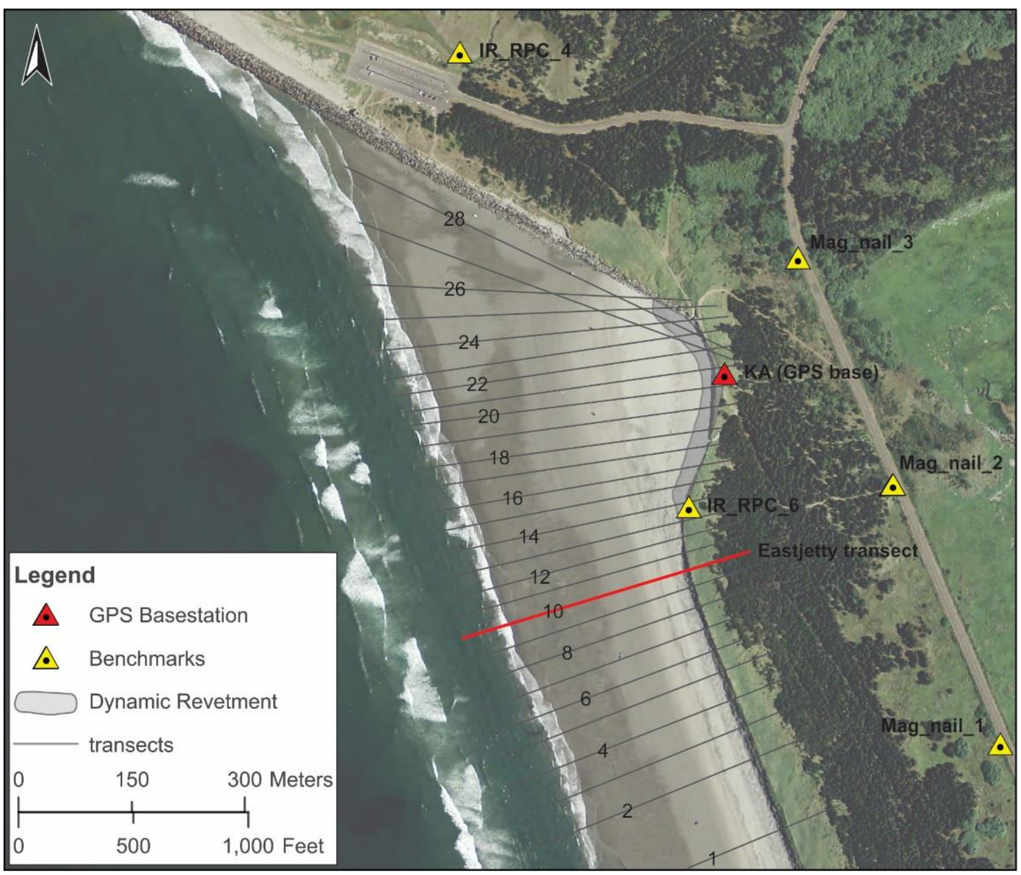

Table 2. Horizontal and vertical coordinates (expressed as a standard deviation) at each of the benchmark locations, compared to the final coordinates referenced in Table 1.

Benchmark Name	Northing (m)	Easting (m)	Elevation (m)
KA	0.010	0.006	0.020
IR_RPC_4	0.008	0.009	0.021
IR_RPC_6	0.000	0.004	0.005
Mag_nail_1	0.003	0.015	0.030
Mag_nail_2	0.000	0.000	0.000
Mag_nail_3	0.018	0.003	0.018

3.1.3 Profile Surveys

For the purposes of this study, we established 28 transects along approximately 780 m (2,560 ft) of shoreline (**Figure 5**). In general, transects north of profile 8 were spaced ~25 m (82 ft) apart; transect spacing is 30 m (98 ft) between profiles 5 and 8, and 40 m (130 ft) south of transect 5. Transects 13 to 28 span the dune area now protected by the dynamic revetment, while transects 27 and 28 provide information specific to the changes occurring at the northern end of the structure. This portion of the structure was established as a sacrificial "feeder" site to the rest of the structure and beach. Finally, transects 1 to 12 span the area covering the natural beach and foredune and thus reflect control sites for changes taking place in the unmodified portion of the beach. Of these, transect 10 (http://www.oregongeology.org/nanoos/data/img/lg/EastJetty_EDA.png) has the longest continuous record of beach and dune changes, dating back to 1997.

After the profile network had been established, the R7 GPS base station was located on the KA benchmark monument (**Table 1, Figure 5**), using a 2.0-m fixed-height tripod. Survey control was provided by undertaking 180 GPS epoch measurements (~3 minutes of measurement per calibration site) using the calibration sites indicated in **Table 1**, enabling us to perform a site calibration that brought the survey into a local coordinate system. This step is important in order to eliminate various survey errors that may be compounded by factors such as poor satellite geometry, multipath, and poor atmospheric conditions, all of which, when combined, can increase the total error to several centimeters. After site calibration was completed, cross-shore beach profiles were measured with the R8 GPS rover unit mounted on a backpack, worn by a mapper. This was undertaken during periods of low tide, enabling more of the beach to be surveyed. **Table 3** documents dates when the beach monitoring sites were measured, along with dates when 3D topographic mapping of the beach were completed.

Table 3. Dates when beach surveys and mapping efforts were undertaken.

Measurement Date	Type
April 1998	lidar
September 2002	lidar
July 2009	lidar
September 2010	lidar
August 7, 2013	contractor survey (pre-construction)
October 8, 2013	RTK-DGPS** (post-construction)
November 14, 2013	RTK-DGPS**
December 11, 2013	RTK-DGPS
January 16, 2014	RTK-DGPS**
March 12, 2014	RTK-DGPS**
September 11, 2014	RTK-DGPS**
December 01, 2014	RTK-DGPS
March 16, 2015	RTK-DGPS**
June 4, 2015	RTK-DGPS**
September 1, 2015	RTK-DGPS**

Note: Asterisks denote those times when 3D topographical mapping was completed.

The approach used to measure the cross-shore beach profiles consisted of walking from the landward edge of the primary dune or bluff edge, down the beach face, and out into the swash zone. A straight line perpendicular to the shore was achieved by navigating along a pre-determined line displayed on a hand-held Trimble TSC2 computer connected to the R8 receiver. The computer showed the position of the operator relative to the survey line and indicated the deviation of the GPS operator from the line. The horizontal variability during the survey was generally minor, typically less than about ±0.25 m either side of the line. This resulted in negligible vertical uncertainties due to the relatively uniform nature of beaches characteristic of much of the

Oregon coast (Allan and others, 2015a). From our previous research at numerous sites along the Oregon coast, this method of surveying can reliably detect elevation changes on the order of 4-5 cm, well below normal seasonal changes in beach elevation, which typically varies by 1-2 m (3–6 ft) (Ruggiero and others, 2005; Allan and Hart, 2007b, 2008).

Analysis of the beach survey data involved a number of stages. The data were first processed in Trimble Business Center (TBC) and then exported in comma-delimited form. The xyz values were then imported into MathWorks® MATLAB® environment (a suite of computer programming languages) using a customized script and further processed. A least-squares linear regression was fit to the profile data. The purpose of this script is to examine the reduced data and eliminate those data point residuals that exceed a ±0.75-m threshold (i.e., the outliers) either side of the predetermined profile line. The data were then exported into a Microsoft® Excel® database for archiving purposes. The data were plotted by using a second MATLAB script with the Excel profile database to plot the survey data (relative to the earlier surveys) and output the generated figure as a Portable Network Graphics (PNG) file. The appendix shows the reduced beach profile plots for the Clatsop Spit transects; these data may also be viewed online via the NANOOS Beach and Shoreline Change mapping portal (http://nvs.nanoos.org/¬BeachMapping).

3.1.4 Topographic Mapping

In addition to the beach profile surveys, topographic 3D surveys of the entire region encompassing the dynamic revetment and subaerial beach down to approximately mid tide level were also undertaken (**Figure 6**); the total area measured using this approach is approximately 330 × 200 m² (1,080 × 656 ft²). This approach is useful for resolving gradients in beach change associated with migrating features such as mega-cusps, sand waves, and rip current embayments. The approach used here was to mount the R8 rover on to the side of a truck by using a specialized GPS truck mount. The height of the GPS above the beach was measured and entered into the TSC2 computer. The vehicle was then driven slowly along the beach, enabling the entire beach to be measured and "filled in" with additional point data (**Figure 6**). In those areas where the vehicle could not go, the R8 rover was mounted on a backpack, worn by a mapper, and the mapper's height measured and entered into the TSC2 computer. The mapper then moved about the area collecting additional points. The data were subsequently processed in TBC and then exported in xyz form to enable additional processing in ArcGIS and in Surfer® (terrain modeler). **Table 3** identifies those dates when topographic 3D surveys were completed on the Columbia River dynamic revetment.

Figure 6. **A topographic 3D survey undertaken on September 1, 2015, showing the spatial distribution of the measurements; in this example 4,369 measurements were made.**

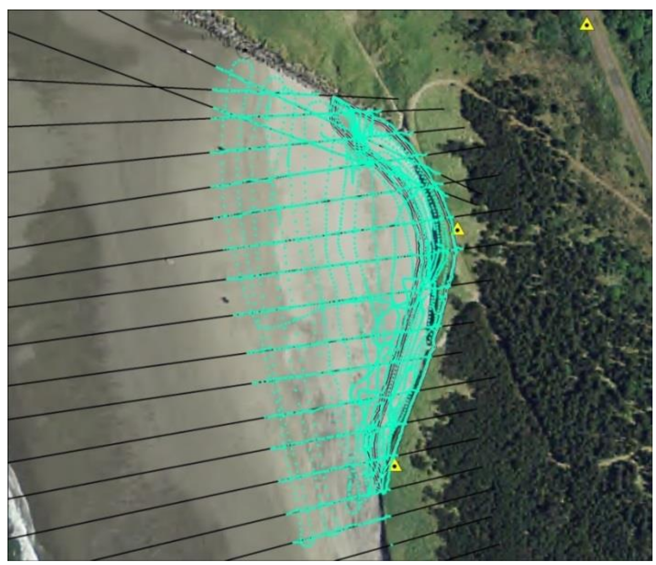

4.0 BEACH PROCESSES ON THE OREGON COAST

4.1 Background

The Clatsop Plains are an arcuate shaped coastline that extends from Tillamook Head in the south to the mouth of the Columbia River (MCR). The plains form part of a smaller subcell (34 km [18.6 mi] in length) located within the much larger Columbia River littoral cell (CRLC), a 165-km (103 mi) coastal system that extends from Tillamook Head, Oregon, to Point Grenville, Washington (**Figure 1**). The Clatsop Plains coastline is characterized by wide, dissipative, surf zones and prominent longshore bars in the nearshore, while the beaches are backed by an extensive dune sequence (Cooper, 1958; Woxell, 1998). The foredunes range in height from ~8 m (26 ft) to over 16 m (52.5 ft). These dunes increase in height from Seaside to just north of Camp Rilea and then decrease in height toward Clatsop Spit (Ruggiero and Voigt, 2000). The beaches are gently sloping (mean slope [tan β] of ~0.040 ± 0.009) and have a somewhat lower beach slope when compared with slopes identified along the Tillamook County coastline (Allan and others, 2015a).

4.1.1 Coastal Change on the Clatsop Plains

For the past several thousand years, the shorelines of the CRLC, including the Clatsop Plains, have been accreting, causing the coastline to prograde seaward by a few hundred to several thousand meters. This process is thought to have begun around 4,000 years ago, as the rate of sea-level rise slowed (Woxell, 1998). Woxell estimated that the Clatsop Plains historically accreted at an average rate of 0.7 m/yr (2.3 ft/yr) from about 4,000 years BP to AD 1700. Between 1700 and 1885, accretion rates along the Clatsop Plains fell slightly to around 0.5 m/yr (1.6 ft/yr).

The year 1885 is significant because this was when construction of the Columbia River south jetty was initiated and the coastline began to prograde seaward by hundreds of meters in response. Change was not constant; response varied in different phases of jetty construction, including the construction of the north jetty, and subsequent maintenance and modification (Lockett, 1963).

Following the building of the south jetty in 1902, Clatsop Spit grew northward by about 4.6 km (2.9 mi) during a period of 50 years. A likely source of the sand that accumulated along Clatsop Spit was due to changes in the Columbia River inlet, which resulted in the development of shoals along the north side of the south jetty, and from erosion of the mid-continental shelf region offshore from the Clatsop Plains (Lockett, 1963; Sherwood and others, 1990). Analyses by Gelfenbaum and others (2001) indicated that between the 1870s and 1926 the mid-continental shelf region and the inlet mouth lost about 364 million m^3 (476 million yd^3) of sand. During this same period, accretion rates along the Clatsop Plains ranged from 2.0 to 5.8 m/yr (6.6 to 19 ft/yr), with an average rate of 3.3 m/yr (10.8 ft/yr). The highest accretion rates were identified near the MCR (Woxell, 1998).

Since the mid-1920s the rate of coastal advance has slowed along the Clatsop Plains. In the far north near the jetty, accretion has been replaced by erosion, which dominated the shoreline response along the northern 4 km (2.5 mi) of Clatsop Spit (**Figure 7**). For example, the north end of Clatsop Spit eroded by some 260 to 300 m (850 to 980 ft) between 1926 and the 1950s, an end-point erosion rate of ~ −11.6 m/yr (~ −38 ft/yr). The erosion of Clatsop Spit was especially significant in the late 1920s. Large damaging storm waves characteristic of the MCR contributed to degradation of the south jetty. The damage culminated with a breaching event through the south jetty in 1928 (USACE, 2013). The large waves also affected the developing foredune next to the south jetty root, which was overtopped and breached (**Figure 8**). As a result of the breach, a large volume of sediment was carried into the lower estuary, changing the inlet's morphology (USACE, 2013). The erosion of the spit tip is probably related to ongoing sediment losses occurring on the mid-continental shelf region offshore from the spit throughout this period, the product of reduced sand supplies from the Columbia River and possible dredging and disposal practices that commenced in the lower estuary. In response to the jetty damage, the USACE initiated a multi-year jetty rehabilitation effort on both jetties, which was implemented in the 1930s and 1940s. Thus, some of the patterns and rates of shoreline change observed during this latter period may be attributed to those efforts to rehabilitate the jetties.

Although the north end of Clatsop Spit was experiencing erosion, the central part of the Clatsop Plains continued to prograde (total accumulation of 60 million m^3 [78 million yd^3] of sand) between the 1920s and 1950s (Gelfenbaum and others, 2001). The pattern of erosion and deposition identified adjacent to the MCR indicate that much of the eroded sand was displaced either seaward or to the north (Lockett, 1963; Sherwood and others, 1990; Gelfenbaum and others, 2001). In particular, the erosion of the outer tidal area provided a large amount of sediment to the littoral system north of the Columbia River, which contributed to significant beach accretion along Long Beach and sedimentation in Willapa Bay on the Washington coast. However, as noted by Sherwood and others (1990), the effects of this large sediment input may now be wearing off.

Figure 7. Shoreline changes adjacent to the Columbia River south jetty from the 1920s to 2009. The location of the constructed dynamic revetment is shown. Red line depicts the location of the Eastjetty profile site (http://www.oregongeology.org/nanoos/data/img/lg/EastJetty.png). Base image is a 2009 orthorectified aerial photograph.

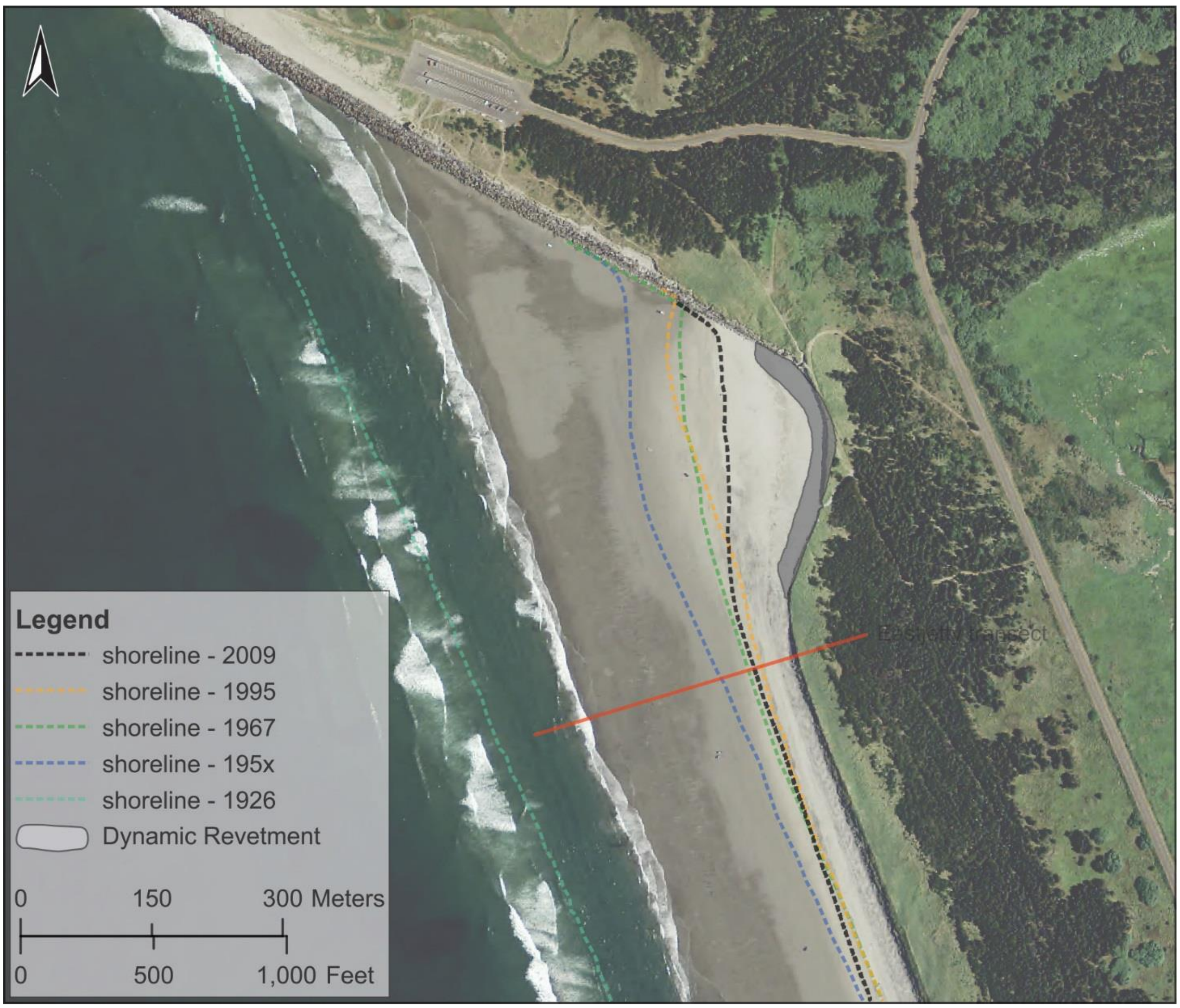

Figure 8. Historical 1928 breaching of the south jetty and adjacent dune system. Top view faces the southeast (USACE, 2013, Figure 2.1).

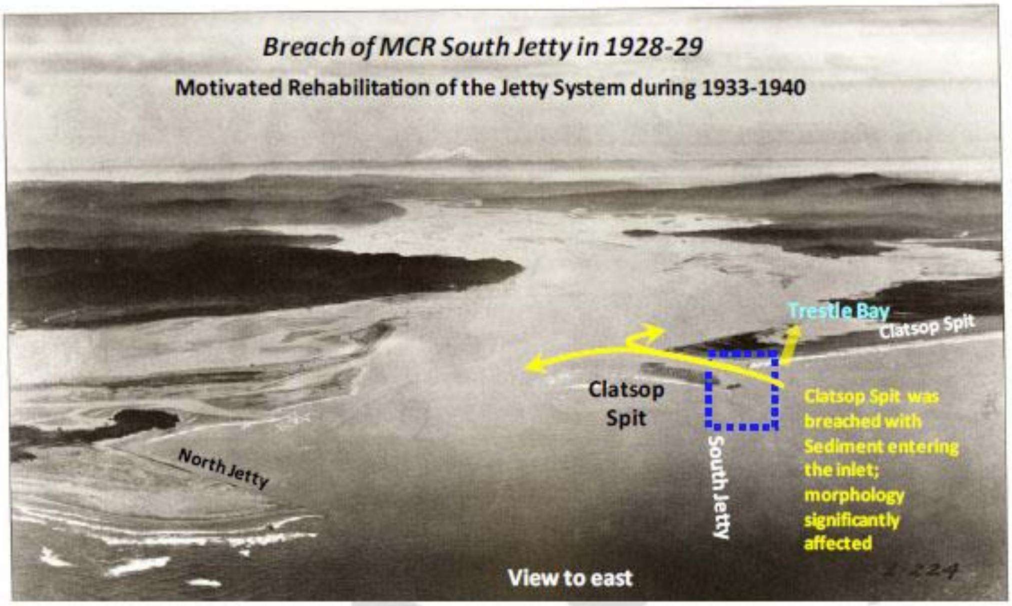

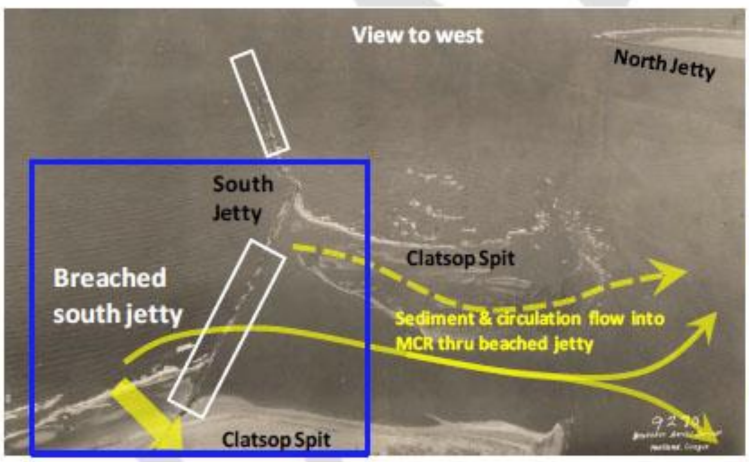

The South Jetty (SJ) was constructed in 1885-1895 to stabilize the highly transient tidal shoals (bar) and establish a deep draft navigation channel through the MCR inlet. During 1903-1913, the SJ was rehabilitated and extend offshore to increase jetty function for stabilizing the inlet.

Figure 2.1, Historical Breaching of the MCR South Jetty. During the 1920's the south jetty experienced severe degradation. By 1928, a breach through the jetty cross-section occurred near the shore connection (root) of the jetty. The consequences of the breached SJ were significant: A Large volume of sediment passed through the breach (from south to north) and deposited within the inlet changing the inlet's morphology. Much of the sediment along the ocean shoreface south of the inlet was transported by flow through the breached jetty (narrowing the margin between ocean Trestle Bay). Storm surge overtopped the shore and passed into Trestle Bay, threatening the stability of the entire inlet. Tidal circulation through the SJ breach promoted the northward migration of Clatsop Spit which adversely impacted navigation through the MCR. The south jetty breach event motivated a 9-year jetty rehabilitation program for the north and south jetties and included the construction of Jetty A.

Recent shoreline change analyses using lidar, aerial photography, and real-time kinematic differential global positioning surveys (RTK-DGPS) of the beach indicate that the north end of the Clatsop Plains is continuing to erode (Ruggiero and Voigt, 2000; Allan and Hart, 2008; Allan and others, 2015a). Erosion is especially acute where the dunes of the Clatsop Plains abut against the South Columbia River jetty (**Figure 7**). For example, between the 1950s and 2009 the shoreline receded by an additional ~96 m (~317 ft) near the south jetty; the erosion rate is estimated to be ~ −1.8 m/yr (~ −5.9 ft/yr) for this period. Repeat seasonal surveys of a beach profile site established next to the south jetty in 1997 (Eastjetty site, http://www.oregongeology.org/nanoos/data/img/lg/EastJetty.png [**Figure 7**]) by staff from DOGAMI indicate that this section of the beach has eroded some 25.6 m (84 ft) since 2000; an ordinary least-squares erosion rate indicates a mean erosion rate of ~ −0.6 m/yr (~ −2 ft/yr), while the end-point erosion rate is higher at ~ −1.7 m/yr (~ −5.6 ft/yr). More recent measurements within the log-spiral curve adjacent to the jetty undertaken by DOGAMI in March 2013 (**Figure 7**) indicate that the dune there has eroded by 30.5 m (100 ft) since 1997.

4.2 The Concept of a Dynamic Revetment

Gravel beaches have long been recognized as an effective form of natural coastal protection, minimizing the potential for inundation from wave overtopping (Bradbury and Powell, 1992; Dornbusch and others, 2002) as well as exhibiting a remarkable degree of stability in the face of sustained wave attack (Nicholls and Webber, 1988; Everts and others, 2002; Allan and Komar, 2004). In part, this response is a function of the coarseness of the particles, which range from 4 mm (−2Ø) to 256 mm (−8Ø), including pebbles to large cobbles. Due to their high threshold of motion and because of the asymmetry of shoaling waves and swash velocities on the beach face, gravels have a greater tendency for onshore movement compared with sand-size particles and can form a steeply sloping gravel beach face (Inman, 1949; Zenkovich, 1967; Horn, 1992). Once formed, the porous gravel beach is able to disrupt and dissipate the incident-wave energy, even during intense storms (Ahrens, 1990; Sherman, 1991; Allan and Hart, 2007a). As a result of these characteristics, artificially constructed gravel beaches have been suggested as a viable approach for protection from coastal erosion and are termed "cobble berms" or "dynamic revetments" when used in such applications (van Hijum, 1974; Ahrens, 1990; Komar and others, 2003; Bird and Lewis, 2015).

The idea of using dynamic revetments for shore protection is a relatively recent approach and represents a transitional strategy between a conventional riprap revetment and a beach nourishment project. The term dynamic revetment highlights this transition in that the gravel and cobbles are expected to be moved by waves and nearshore currents, whereas a conventional "static" riprap revetment using boulder-size quarry stone is designed not to move (Ward and Ahrens, 1991). In this regard, the cobble berm is constructed to provide protection to coastal developments while remaining more flexible than a conventional riprap revetment, adjusting rather than failing when movement occurs. Dynamic revetments can front directly into the water (Loman and others, 2010) or can be located landward of a sandy beach that is providing inadequate buffer protection from erosion by waves and currents (Allan and Komar, 2004). Such morphologies are relatively common on some coasts, so the placement of a cobble berm constitutes a more natural and aesthetic solution than a conventional riprap revetment or seawall. The objective is to construct the cobble berm to be as close as possible in form and behavior to natural gravel beaches in order to be compatible with the natural environment and to insure stability.

The origin of the use of dynamic revetments for shore protection is uncertain. Early papers on the artificial nourishment of gravel beaches describe geomorphic characteristics that are similar to those for a cobble berm (Muir Wood, 1970). The concept of a structure having a dynamic response to wave attack on a larger scale has also been applied to rubble-mound breakwaters (Bruun and Johannesson, 1976; Willis and others, 1988). The earliest published paper that considers the design of an artificial gravel beach is that of van Hijum (1974), who described the application of gravel along the bank of the entrance to Rotterdam Harbor, Netherlands, more to dissipate wave energy rather than to serve as shore protection. A similar engineering application is that of Ahrens (1990), who studied the use of a constructed cobble berm to protect a bulkhead located in shallow water.

There are a number of practical advantages in using a cobble berm for property protection (Ahrens, 1990; Ward and Ahrens, 1991):

- Smaller stones are typically less expensive than large armor stones used in a conventional riprap revetment;
- Placement of the material does not require special care. As a result, the boulders may be dumped at the site rather than individually placed, making the construction process much simpler;
- Movement of the gravels by ocean processes does not constitute failure but is desirable in that the gravel berm adjusts its shape to reflect the predominant storm wave conditions; and,
- Dynamic revetments are more aesthetically acceptable when compared with a conventional seawall or riprap revetment because they the appearance of natural gravel beaches. This may make construction more acceptable by management authorities, even on coasts that do not permit the use of conventional “hard” structures.

Constructing a dynamic revetment requires more material than does a riprap revetment, but the dynamic revetment is generally less expensive than “hard” engineering structures. Nevertheless, it cannot be expected that a dynamic revetment will provide the same level of shore protection as a conventional riprap revetment or seawall. The gravels can be moved by the waves, and the placed material may be transported alongshore or offshore by extreme storm waves (Allan and others, 2006). Thus, maintenance requirements can be expected to be more frequent than for static structures.

4.2.1 Examples of Dynamic Revetment Construction

Globally, there are relatively few examples where dynamic revetments have been constructed, and many of these occur in relatively low-wave-energy environments. For example, (Downie and Saaltink, 1983) describe the construction of a dynamic revetment along the shore of Vancouver, British Columbia. The site is characterized by a pocket beach backed by high cliffs (~61 m [220 ft] high) that had experienced rapid erosion. A dynamic revetment was chosen for the site; this choice reflected a compromise between engineering needs and the needs of local beach users. The completed structure was found to perform well, with the cobbles generally remaining on the upper beach face. However, over time much of the gravel was removed along the shore out of the design area.

There are numerous examples of dynamic revetments having been constructed around the shores of the Great Lakes (Johnson, 1987). Initially, the structures were constructed inadvertently, having formed from the erosion and redistribution of copper mine tailings. As the gravel beaches grew, erosion hazards were subsequently reduced, leading to an expansion of their application around the shores of the Great Lakes.

At Flathead Lake in Montana, a 60-m-long dynamic revetment was constructed to mitigate an erosion hazard problem. The structure consisted of a base of boulders and cobbles, which was overlaid with additional cobble to form a sloping gravel beach face (Lorang, 1991). The completed structure performed well, effectively reducing the erosion hazard, although the site did experience some loss of gravel due to the oblique wave approach characteristic of the lake and field site.

At Washdyke beach in South Canterbury, New Zealand, a type of dynamic revetment was built to provide short-term erosion relief to an area adjacent to an existing ocean outfall, while a new outfall was built elsewhere (Kirk, 1992). The temporary constructed gravel berm was 300 m long and was centered on the outfall. The structure was built in two phases. Phase 1 reflected the relocation of gravel that had washed over onto the landward side of the barrier beach, raising the crest elevation of the beach by about 2–2.5 m (6.5–8 ft). Phase 2 consisted of the addition of 9,800 m^3 (~12,800 yd^3) of coarser gravel, which was used to cap the reconstructed barrier. According to Kirk, the reconstructed barrier beach was extremely successful, reducing the overall erosion rate by 55% over a period of 5 years, with no crest retreat and no overtopping.

Recently, a dynamic revetment was constructed at Cape Lookout State Park (CLSP) in Tillamook County, Oregon (Allan and Komar, 2002a, 2004; Allan and others, 2006; Allan and Hart, 2007a). The structure was built to combat extensive erosion of the primary dune, which separates the beach from a campground located immediately landward of the eroding dune. The structure was completed in two phases. Phase 1, initiated in summer 1999, consisted of the installation of an artificial dune built from sand bags, while Phase 2, construction of the cobble berm, was completed in December 2000. Gravel was extracted from the natural cobble beach in the north along Netarts Spit (~3,000 m^3 [3,924 yd^3]) and from the south end (~2,300 m^3 [3,008 yd^3]) of the cell in areas where it was believed that more than sufficient volumes were present to protect the dunes and where no park infrastructure was present. The cobbles were carried to the construction site on a front loader and were placed evenly across the pre-existing profile. The volume added along the length of the constructed dynamic revetment varied depending on the antecedent beach morphology. The artificial dune was overlaid with a jute coconut fiber cloth, on which native grasses were planted.

Since its construction, the CLSP structure has withstood multiple large Pacific Northwest winter storms, including several events that led to the structure being overtopped (Allan and Komar, 2004; Allan and Hart, 2007a). Despite evidence for significant cross-shore gravel movement, successive beach profile surveys and cobble tracing experiments undertaken over several years confirmed the basic premise that the gravels tended to remain on the structure, migrating landward up on to the gravel berm during storms (Allan and others, 2006; Allan and Hart, 2007a). This last response is consistent with both field-based observations (e.g., Everts and others [2002]) and studies undertaken with wave flumes (Loman and others, 2010; Van der Werf and Van Gent, 2010). Nevertheless, Allan and others (2006) identified a prevailing northward movement of cobbles, which suggested that in time the structure would require periodic remediation to counter the loss of cobbles to the north. The latter issue has indeed occurred such that the Oregon Parks and Recreation Department (OPRD) has had to add additional cobbles to the dynamic revetment at least three times during the last decade. These later efforts have included the relocation of existing cobbles accumulating to the north of the structure and their removal to the south, as well as introduction of entirely new material to the cobble berm.

At the Port of Rotterdam, Netherlands, a dynamic revetment gravel beach has been built seaward of a new port expansion (Loman and others, 2010). The gravel beach was perched on sand and was fronted by a boulder reef. The design concept was extensively tested in large flumes and was found to stand up very well to extreme wave and water level conditions.

4.2.2 The Columbia River Dynamic Revetment

August-October 2013, the USACE Portland District constructed a dynamic revetment next to the Columbia River south jetty. The purpose of this structure is to mitigate ongoing erosion of the primary dune adjacent to the south jetty root (**Figure 2**) and, ultimately, to prevent the dune from being breached. The structure is approximately 335 m (1,100 ft) in length (**Figure 10**). The Columbia River dynamic revetment is bounded in the north by the south jetty; in the south the structure tapers into the existing natural dune to minimize the potential for flanking (**Figure 10**). This last feature also serves to minimize other potential adverse "end effects" that may result from wave-current interactions (strong on-offshore currents, wave reflection, and alongshore currents) on the structure and the transfer of those processes to the natural dune, where they may cause enhanced erosion.

Figure 9. Looking south along the completed dynamic revetment structure. The dark banding near the center of the structure is angular quarry rock that has been established to enable vehicle access to the beach (photo: J.C. Allan, DOGAMI, October 2013).

Figure 10. Schematic map showing the spatial characteristics of the completed structure, including the locations of various key morphological features.

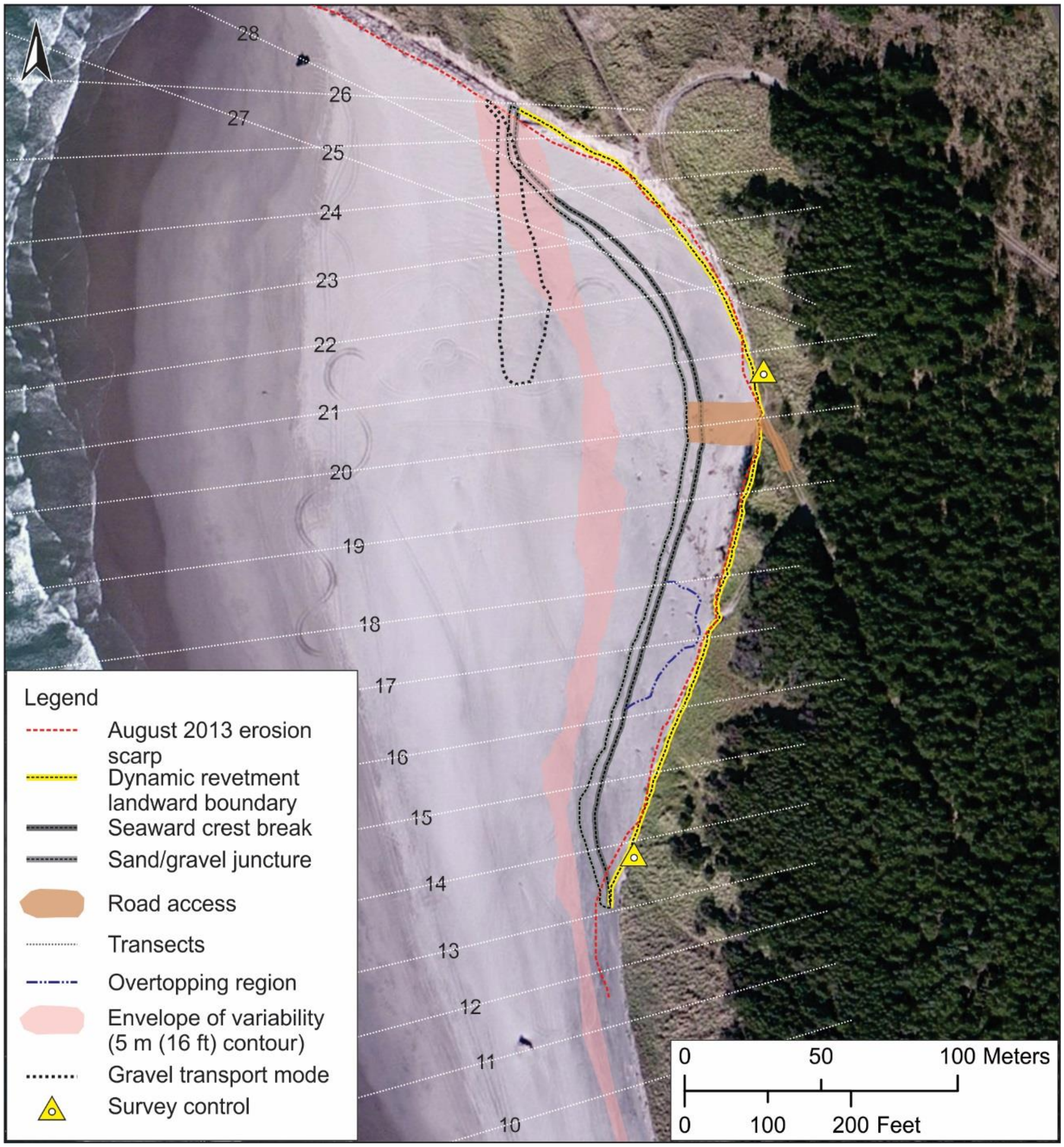

Allan and others (2005) noted several important variables when designing a dynamic revetment: predominant size of the gravels (plus sorting and shape), slope (a function of the predominant grain-size), crest elevation, width of gravel berm, and berm volume. The final design of the Columbia River dynamic revetment by the USACE was determined from a combination of these variables and from previous investigations of dynamic revetments, morphological observations of naturally occurring gravel beaches present on the Oregon coast, repeat measurements of profile changes measured at the Eastjetty transect (**Figure 7**) located near the south jetty, and wave runup calculations under varying storm scenarios. The final design metrics (**Figure 11**) included the following.

- An initial design slope was established at tan β = 0.2 (1v:5h); the slope is expected to change over time. The minimum equilibrium beach slope expected is likely to be approximately tan β = 0.067 (1v:15h). The USACE recognized that once completed, the structure is likely to be periodically covered with a thin veneer of sand, especially in the summer when wind-blown sand is carried onto the structure;
- Critical for defining the structure's crest elevation was an analysis of the wave runup superimposed on the tide. Modeling by the USACE indicated a preferred crest elevation of 6.7 m (22 ft). This event has a return period of ~10–20 years, depending on which storm tide level is used;
- The width of the cobble berm at its crest was established at 19.8 m (65 ft) (**Figure 10** and **Figure 11**);
- The structure would be built in three gravel layers;
- A lower bedding filter layer, approximately 0.6 m (2 ft) thick, was established on the sandy beach. These gravels consisted of angular gravels that were less than −4.7Ø (25.4 mm [1"]) in size. Up to 6,100 m^3 (8,000 yd^3) of gravel is estimated to make up this layer;
- Above the lower layer is a central cobble layer constructed using angular material. The specified size range was established at −4.7Ø to −7.7Ø (25.4 to 203 mm [1" to 8"]), although the gradation used was skewed to coarser cobbles, with more than 50–70% of the cobbles passing a −6.7Ø (102 mm [4"]) screen. The USACE observed that once exposed, the angular cobbles should become sub-rounded in 2–5 years, depending on the frequency of wave action. Approximately 13,762 m^3 (18,000 yd^3) of cobble is estimated for this layer;
- An upper cobble layer, approximately ~1.2 m (4 ft) thick, overlays the core layer. The cobble size range in this layer was established at −4.7Ø to −7.7Ø (25.4 to 203 mm [1" to 8"]), with a mean size of ~-6.5Ø (~90 mm [3.5"]). These cobbles are rounded in order to maximize porosity and thereby reduce the potential for wave runup. Approximately 13,762 m^3 (18,000 yd^3) of cobble is estimated for this layer;
- As part of the construction, the USACE indicated that up to 13,762 m^3 (18,000 yd^3) of sand was expected to be excavated in order to establish the toe of the structure below the eroded winter profile (**Figure 11**); analyses of beach profile changes at the Eastjetty transect revealed that the winter profile is typically about 1–2 m (3–7 ft) below the summer profile. Once the structure was built, the excavated sand would be piled back onto the seaward slope of the gravel berm.

Figure 11. The Columbia River south jetty dynamic revetment conceptual design (after USACE, 2013).

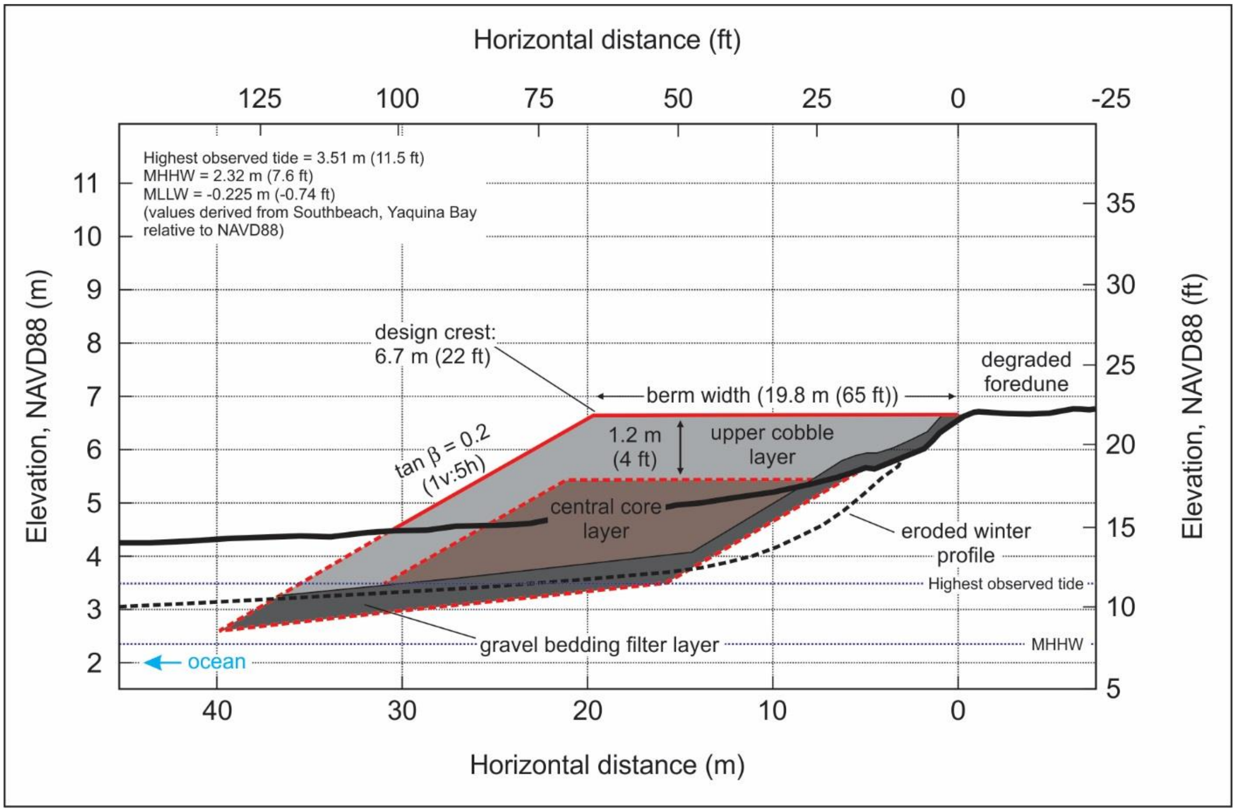

Additional analyses indicate that the structure may require periodic gravel "top-ups" on an approximately 10-year basis to maintain the structure's overall integrity (USACE, 2013). This is because the far north end of the structure could experience some 30–76 m (100–250 ft) of recession over the 10-year period due to sediment transport processes, which will redistribute some of the gravel to the south. From this estimate, the dynamic revetment may require some form of maintenance every 10–15 years for 60–150 m (200–500 ft) of the total structure length. Much of the gravel replacement could be achieved by simply relocating the displaced gravel, in order to fill in those areas that sustain some loss. Estimates of the volume of gravel needed range from 3,000 to 7,600 m^3 (4,000 to 10,000 yd^3) for every 10-year period throughout the project life-cycle. This is a conservative maintenance estimate, based on assumed high rates of gravel displacement. The minimum required life-cycle for this project feature is 30 years; expectations are that an effective life-cycle of 50 years may be realized if the project is adequately maintained. According to the USACE (written communication, 2013), maintenance of the structure will be triggered when the crest width of the structure has been reduced to less than 3 m (10 ft) along a continuous reach of more than 60 m of the structures length (200 lineal ft). At this point, the revetment cross-section loses its ability to protect the foredune and backshore from events greater than the 10-year event, leading to potential erosion and loss of the foredune. Additional maintenance consideration may needed for areas of the project where vehicle access is accommodated over the revetment crest and onto the beach.

5.0 RESULTS

Figure 10 provides a map of the completed structure, showing its overall spatial configuration. Identified on the map is the landward extent of the eroded dune just prior to beginning construction of the dynamic revetment, the crest break that marks the transition from the gently sloping structure crest to the steeper seaward face of the gravel berm, and the location of the sand/gravel juncture as measured in late October 2013 (**Table 3**). Also identified in **Figure 10** is a depiction of the envelope of beach variability measured at the 5 m (16.4 ft) contour elevation. This region of variability was derived from all survey information and shows the landward and seaward extent of changes measured at this elevation. These changes are the product of variations in the seasonality of the waves, as well as the effect of storms. As can be seen in **Figure 10**, the greatest excursions occur at the north end of the structure, where it is currently eroding. Further descriptions of these responses are provided in more detail below.

5.1 Beach Profile Morphological Changes

Beach profiles provide important information concerning the temporal (time) and spatial (cross-shore) variability in the shape of a section of beach. The information derived from repeated surveys provides a measure of the response of the beach to variations in wave energy (e.g., summer versus winter wave conditions), which is reflected in accretion of the beach during the summer and erosion in winter. These data may also contain important information on how the beach responds to major storms, including erosion of the dynamic revetment and adjacent natural dune control sites. Results from beach monitoring are provided in the appendix and are posted online (http://nvs.nanoos.org/BeachMapping). Given the relatively short period in which the profiles have been observed in the study area, information determined from previous light detection and ranging (lidar) topographic surveys has also been used to supplement the GPS-measured beach monitoring data. In addition, we have incorporated topographic measurements undertaken by the USACE engineering contractor in order to document the beach conditions in the vicinity of the dynamic revetment immediately prior to its construction. These latter data are especially useful for documenting the extent of the beach and dune erosion as of August 2013 and are included in **Figure 10**.

Beach morphological changes for four representative study sites (CR_USACE16, -20, -24, and -28) located in the area protected by the dynamic revetment are presented in **Figure 12**, and their locations are identified in **Figure 5** and **Figure 10**. In addition, **Figure 13** presents a summary of the intersurvey changes, expressed as contour changes determined at the 6 m (19.7 ft) elevation, for all affected transects that cross the dynamic revetment. In all cases, the changes are relative to the position of the beach as of April 1998 and reflect horizontal adjustments in the position of the beach relative to this position. As a result, negative sloping lines in **Figure 13** indicate erosion, while positive sloping lines indicate accretion. Yellow circles in the figure denote the position of the beach at the time the structure was completed. Thus, the abrupt seaward (right-hand) shift in the position of the contour between August and October 2013 coincides with the “nourishment” of the beach and the completion of the dynamic revetment.

The four profile examples presented in **Figure 12** highlight the degree of beach and dune erosion that has occurred near the south jetty since the late 1990s, evident by the shifting positions of the beach profile in 1998, 2009, and 2013. Not surprisingly, erosion has been significant in all areas covered by the embayment. In general, transects 15–19 indicate persistent erosion having taken place between 1998 and 2013, with the erosion having been sustained up to when the structure was built. This relatively continuous period of erosion is identified in **Figure 13** by the near linear trend in the pattern of erosion identified between 1998 and August 2013. This contrasts with the response observed north of transect 18, where the bulk of the erosion appears to have occurred since 2002; as can be seen in **Figure 13**, north of transect 18 the beach profiles accreted slightly following the 1997-98 El Niño winter.

Figure 12. Morphological changes observed at four of the Columbia River south jetty dynamic revetment beach cross-section sites. Dark gray shading denotes the normal range of sand variability, while the light gray documents the maximum/minimum elevation changes. Dashed line denotes the position of the beach in August 2013, immediately prior to construction of the dynamic revetment.

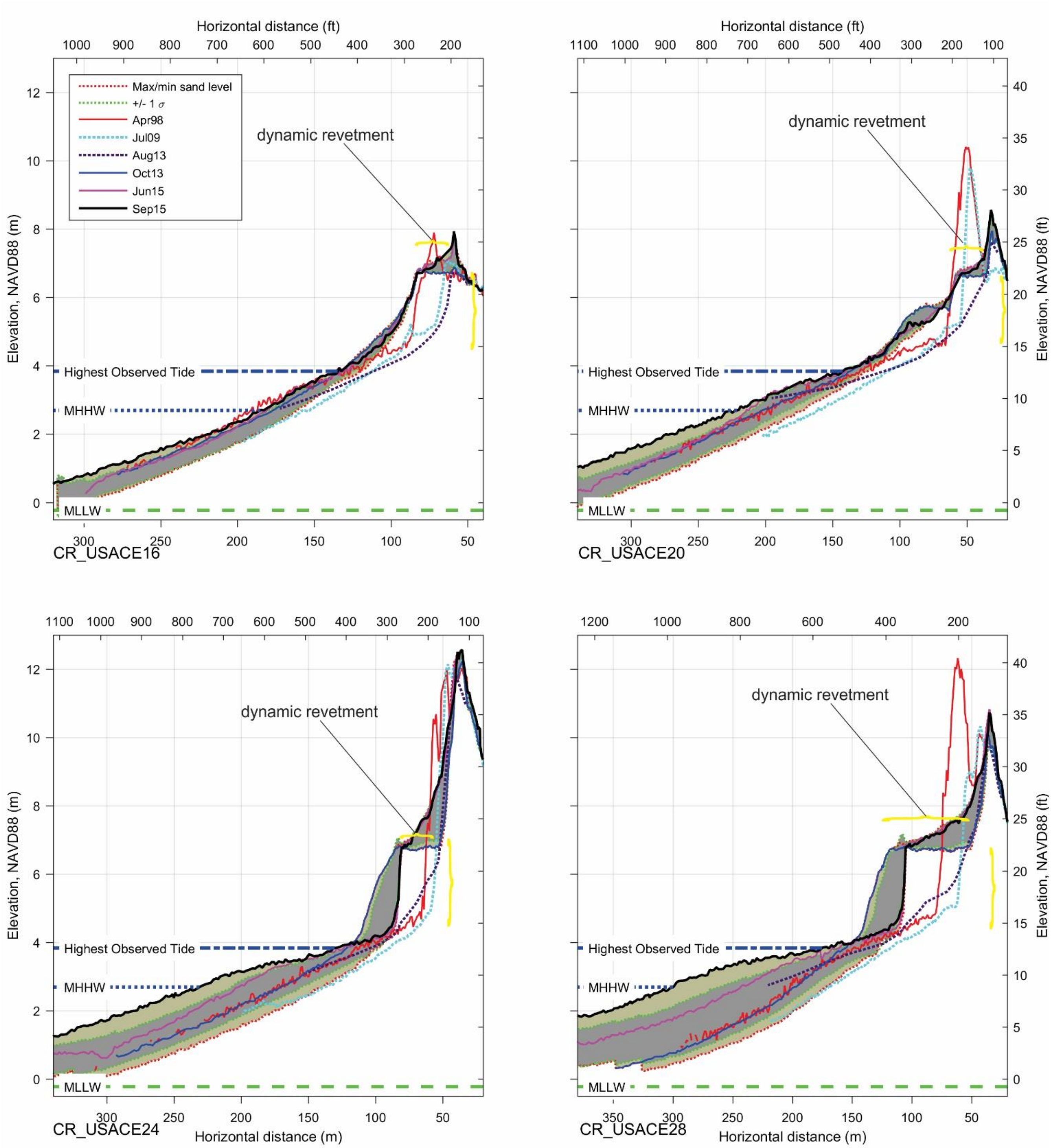

In the south at transect 16 (CR_USACE16, **Figure 12**), the original dune reached heights of ~8 m (26 ft), which progressively increased to the north (10.5 m (34.5 ft) at CR_USACE20, 12.6 m (41.3 ft) at CR_USACE24, and 12.3 m (40.4 ft) next to the south jetty). Today the foredune crest heights tend to be lower: 7.9 m (26 ft) at CR_USACE16, decreasing to 10.7 m at CR_USACE28, while in a few areas near the central part of the structure the dune has shifted landward (e.g., transects 16–18, appendix). This latter response is largely due to aeolian processes carrying sand into the backshore, where it is trapped by European beachgrass. The lowest dune heights today are located between transects 14 and 18. As can be seen in **Figure 12** and **Figure 13**, the abrupt seaward shift in the profile contours (from elevations 4 m to 7 m [13 ft to 23 ft]) reflects the completion of the dynamic revetment in late October 2013.

Figure 13. Time stack of changes at the 6 m (19.7 ft) contour elevation for transects than span the dynamic revetment. All changes are relative to the position of the beach in 1998. Negative sloping lines indicate erosion, while positive sloping lines are indicative of accretion. Yellow circles indicate the position of beach at the time of completion of the dynamic revetment. Red dots denote the time of the survey.

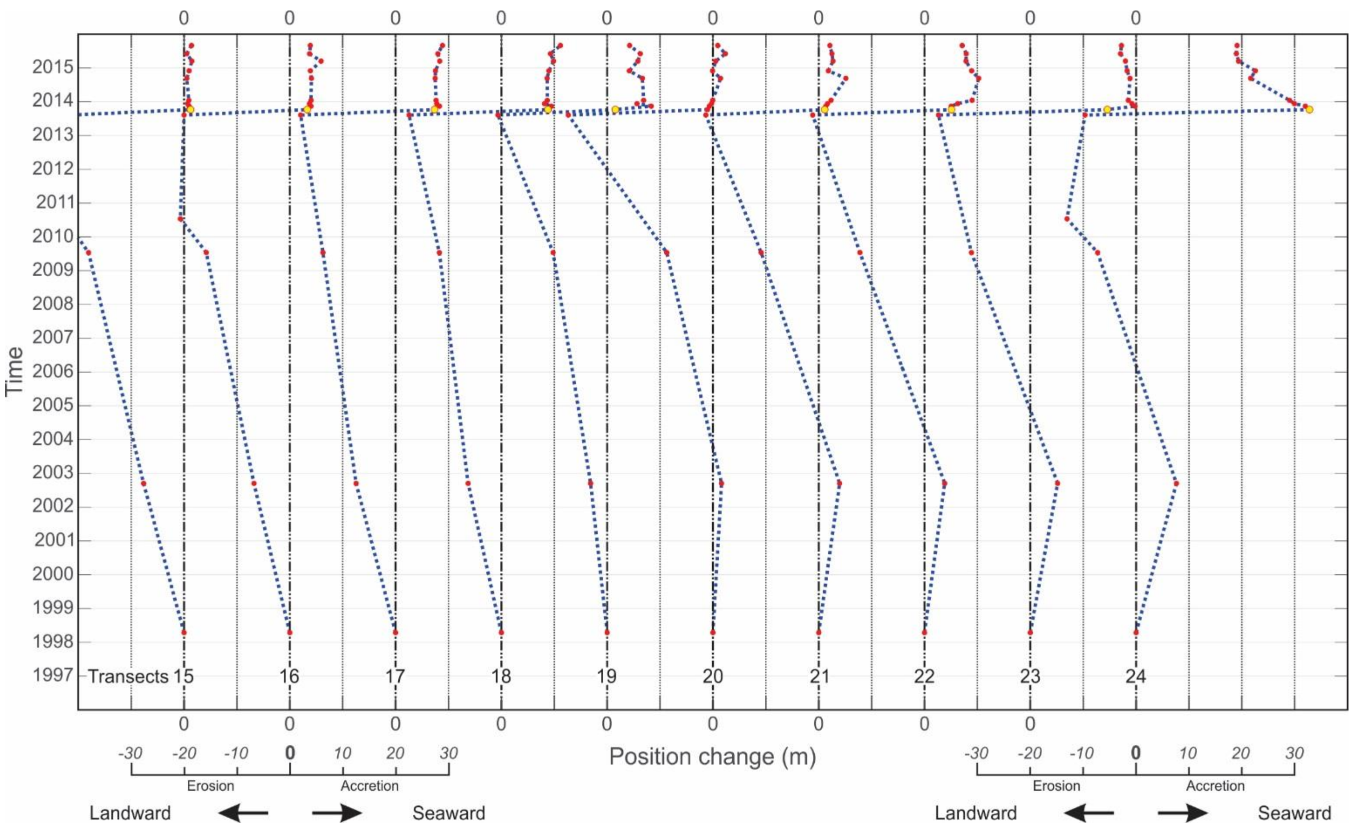

The overall morphological response of the dynamic revetment to wave and current processes to date can largely be divided into two regions. South of transect 20, the morphology of the structure has experienced little to no change to its seaward gravel face. Overall, this section of the gravel berm has experienced minor sand aggradation up against the structure's seaward face, evident by the generally positive changes in the time stack plot presented in **Figure 13**, and in the juncture between the gravel berm and the remnant dune (**Figure 12**). Nevertheless, between transects 16 and 18, the structure crest was overtopped during a moderate storm on January 12, 2014 (**Figure 14**). This event represents the only known event to have overtopped the structure to date. The structure did not experience any erosion between transects 16 and 18 due to the storm, although the gravel berm was eroded in the north.

Figure 14. An overtopping event on the Columbia River south jetty revetment January 12, 2014. A) Minor flotsam was carried up to the crest of the dynamic revetment. B) The spatial extent (red outline) of the overtopping event (photo: J.C. Allan, DOGAMI, January 2014).

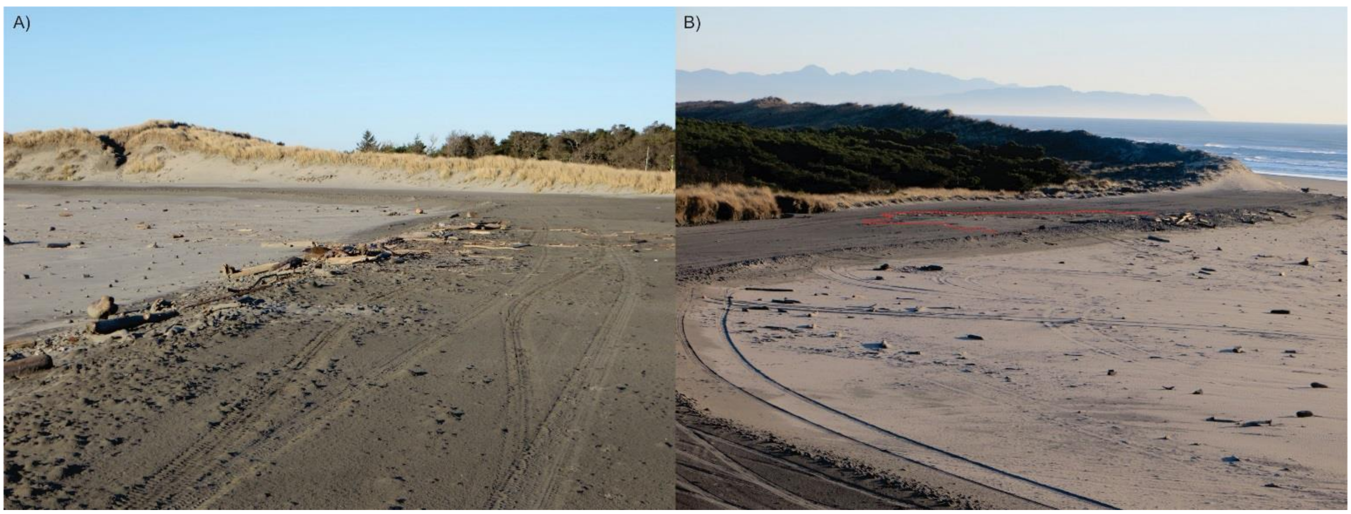

Along the distal north end of the gravel berm, the structure has experienced a significant amount of erosion, which resulted in the development of a prominent erosion scarp shortly after construction of the gravel berm (**Figure 15**). Recall, that this portion of the structure is considered to be sacrificial material and is expected to erode landward over time. At transect 24, the gravel berm has eroded by 13.7 m (45 ft) since October 2013 (**Figure 13**) and by as much as 15.7 m (51 ft) at transect 25. When measured parallel to the south jetty (i.e., transect 28), the dynamic revetment has eroded landward by 20 m (65.6 ft). The bulk of this erosion took place over the initial 2013-14 winter, and slowed slightly over the 2014-15 winter.

Finally, the entire length of the structure crest has experienced significant accumulation of wind-blown dune sand, which has piled up against the juncture of the original dune and structure. This response is most apparent in the area between transects 24 and 28 (**Figure 12**) and can be clearly seen in **Figure 15**.

Figure 16 highlights the broad morphological characteristics of the natural dune in the study control area south of transect 11. Dune crest heights throughout this area decrease from south to north, from a high of 14.6 m (48 ft) at transect 1 to ~10.5 m (34 ft) at transect 10 (see appendix plots). As can be seen in the appendix plots, erosion of the natural dune has been significant in the past, particularly north of transect 3. However, these responses reflect changes that have taken place between 1998 and 2010. Since 2010, the beach and dunes have experienced essentially little to no erosion. In fact, repeat seasonal monitoring of the Eastjetty transect site (http://www.oregongeology.org/¬nanoos/data/img/lg/EastJetty_EDA.png; CR_USACE10) by DOGAMI staff indicates that this site has remained stable since about 2010 and in fact has accreted slightly over this period; prior to 2010 the beach and dune were actively eroding landward. This lack of erosion is largely due to the fact that there have been no significant storms during this time period.

Following construction of the dynamic revetment, our monitoring and beach analyses to date show no evidence for a negative response at any of the study control sites. Furthermore, immediately adjacent to the south end of the structure (near transect 11) where "end effects" might be observed, our measurements indicate no adverse response, with the beach and dune having gained sand over this period and, most recently, gravels that have been transported along the toe of the dune.

Figure 15. Erosion of gravels at the distal north end of the structure (bottom of photo) are currently being transported south along the beach. The photo view is toward the south. Note the aggradation of sand taking place on top of the structure due to aeolian processes (photo: J.C. Allan, DOGAMI, March 2014).

Figure 16. Morphological changes observed at two representative beach profile sites located within the study control area. CR_USACE10 is located immediately adjacent to the south end of the dynamic revetment, while CR_USACE2 is near the far southern end of the control area.

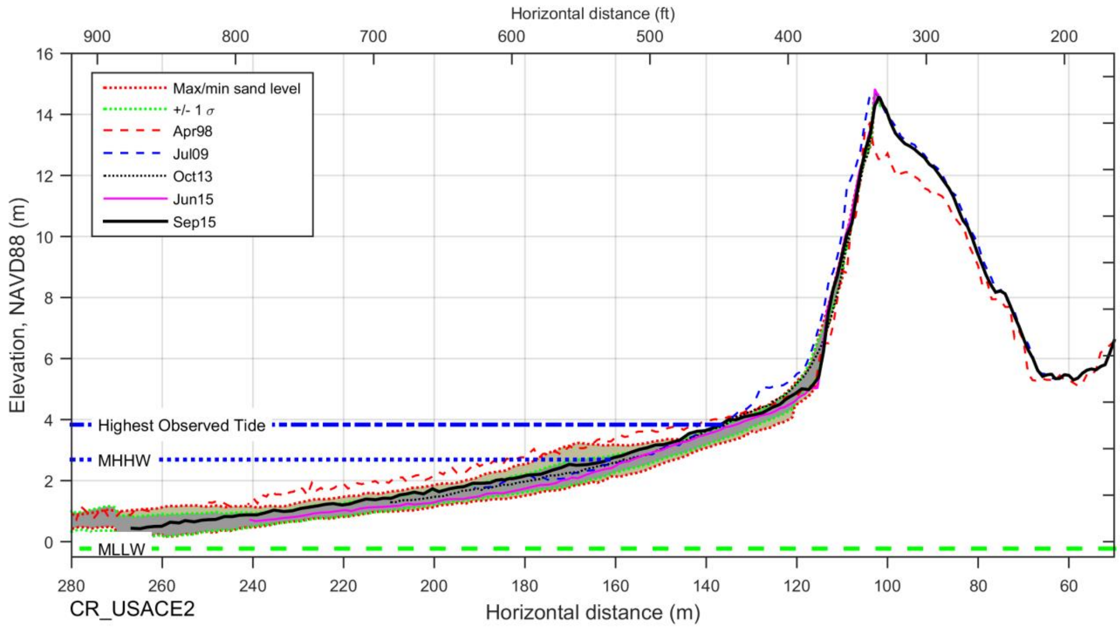

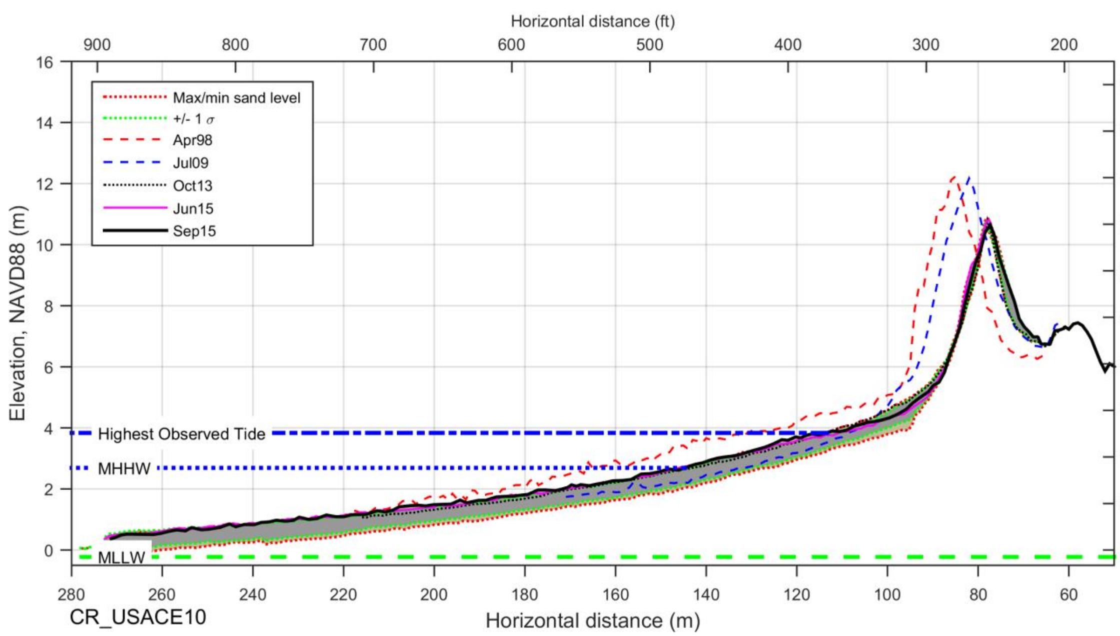

5.2 Topographic 3D Changes

Topographic changes measured by mounting the GPS on a truck are presented in **Figure 17** for selected intersurvey periods. Aside from some early erosion at the north end of the dynamic revetment, the first intersurvey period between October and November 2013 is characterized by a slight lowering of the seaward beach face, while much of the structure experienced little to no change. Between November 2013 and January 2014, erosion of the distal end of the structure becomes more pronounced. During this period, the seasonal decrease in the elevation of the beach face typical of the transition to winter conditions can be clearly seen. On the structure itself, there is generally little observed change, other than at the north end of the gravel berm where sand begins to aggrade up against the natural dune. **Figure 15** also shows this last response taking place. Between January and March 2014, the northern end of the structure continues to erode, while the south central region shows small amounts of aggradation.

From March to September 2014 (**Figure 17**), the measured changes largely reflect rebuilding of the intertidal beach following the end of winter storm waves and the switch to smaller west to northwesterly swell waves, typical of the summer. These latter conditions tend to drive sand back onto the beach face, effectively causing it to aggrade. Minor erosion and accretionary responses observed along much of the structure probably reflects the sand that is being transported by wind. Nevertheless, the structure did experience some additional minor erosion at its north end between March and April, 2014.

The 2014-15 winter is depicted by the changes observed between September 2014 and March 2015 (**Figure 17**). As can be seen, the beach generally experiences little change throughout this period, other than some additional erosion in the north up against the south jetty, while accretion characterizes the south central portion of the beach. As will be discussed below, this lack of response is not surprising given the extremely mild winter wave conditions observed during this period. Finally, the period between March and September 2015 again captures the seasonal aggradation of the beach as post-winter waves change to smaller summer waves and sand is transported from offshore bars back onto the subaerial beach.

Figure 18 presents the net changes measured between October 2013 and September 2015. Included in the figure are contour changes measured at the 5 m (16.4 ft) elevation. These data better depict the horizontal shoreline responses and further highlight the truncation of the structure at its north end. Overall, **Figure 18** (left) highlights the two most significant morphological responses observed of the structure to date:

1. Erosion and truncation of the north end of the structure, which has eroded landward by about 20 m (65.6 ft) as measured at transect 28, which is orientated parallel to the south jetty; and,
2. Aggradation of sand taking place up on the structure crest, up against the original dune line.

With these data we can estimate the net volume change across the structure, which amounts to a net loss of ~2,300 m^3 (3,000 yd^3) of material to date. All of this loss can be attributed to erosion taking place at the north end of the gravel berm.

Figure 17. Topographic 3D measurements of beach changes measured for select intersurvey periods at the Columbia River south jetty dynamic revetment.

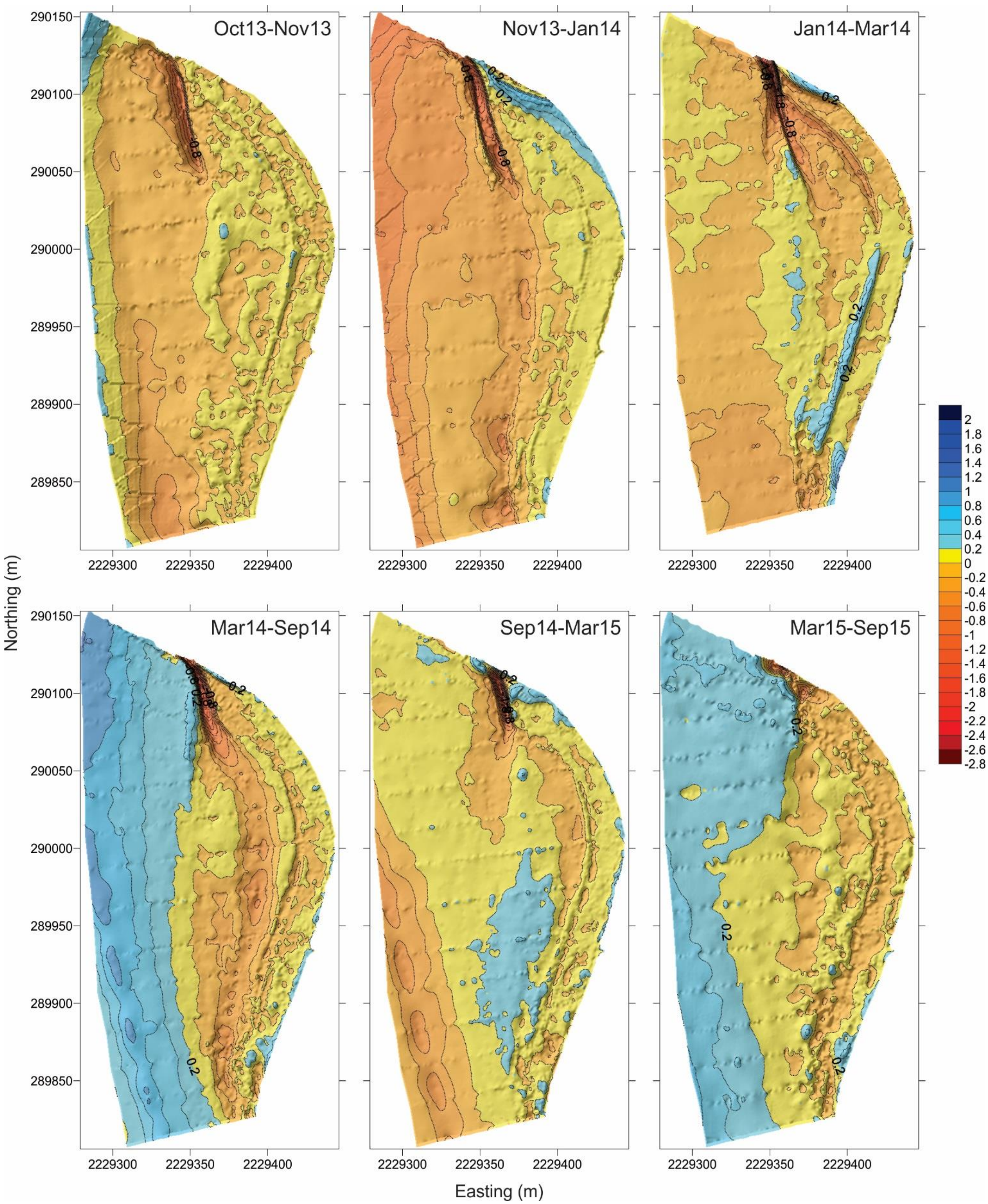

Figure 18. Net 3D topographic beach changes at the Columbia River south jetty dynamic revetment. Left) Contour and topographic elevation changes between October 2013 and September 2015. Right) Contour changes measured at the 5 m (16.4 ft) elevation for all surveys.

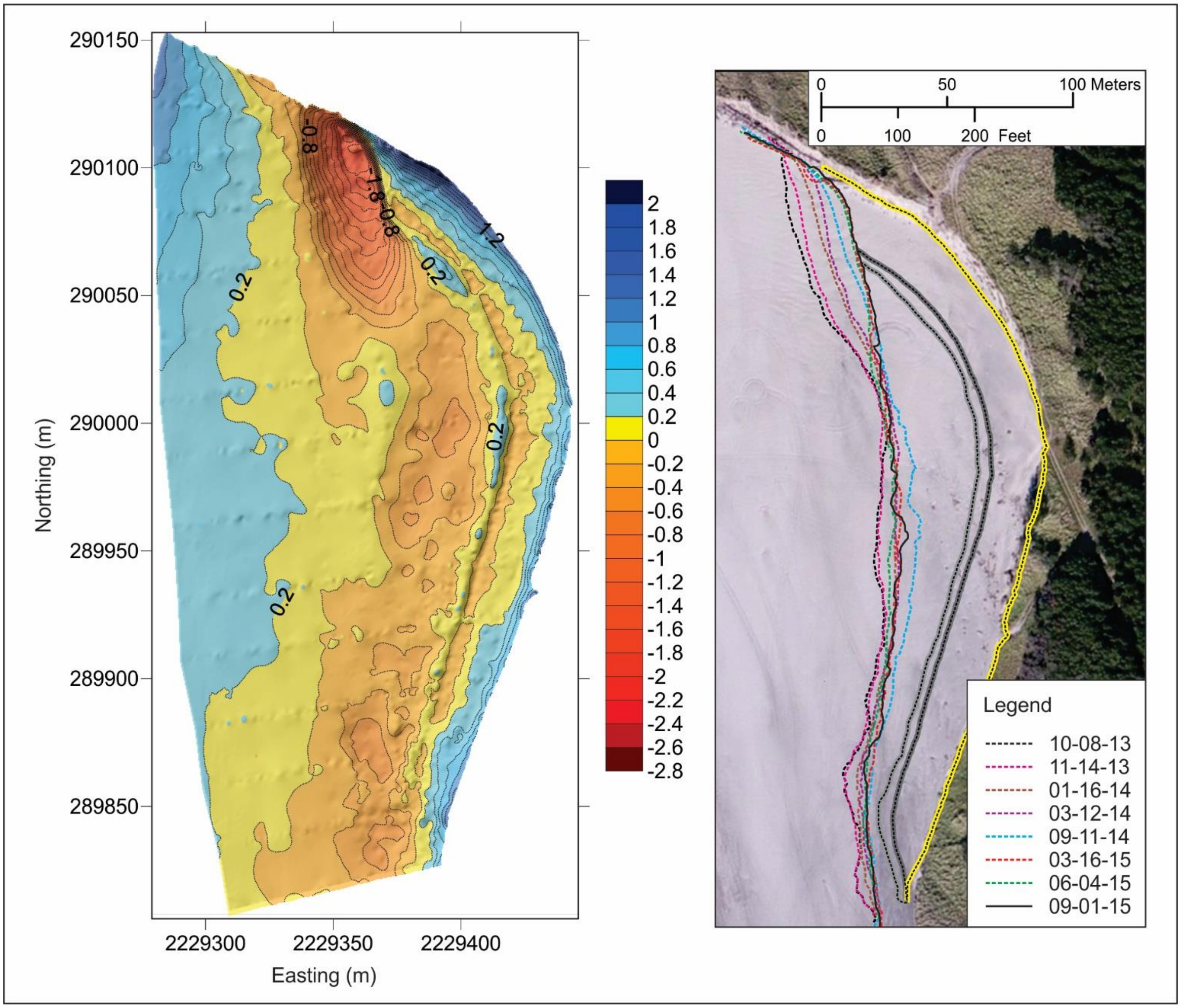

5.3 Physical Processes

Finally, we present a brief assessment of the wave and tide conditions measured over the study period, especially in the context of a much longer, 39-year, wave record. National Data Buoy Center (NDBC) wave buoy data measured at the Tillamook (#46089) (http://www.ndbc.noaa.gov/station page.php?station =46089) and Oregon (#46002) (http://www.ndbc.¬noaa.gov/station page.php?station=46002) sites were obtained from NOAA, along with water levels measured at the Garibaldi tide gauge station (#9437540). (http://www.co-ops.nos.noaa.gov/waterlevels.html?¬id=9437540). These latter data were obtained from the National Ocean Service (NOS) and provide an excellent assessment of tide conditions along the open coast (Allan and others, 2015b). Both the NDBC 46089 buoy and Garibaldi stations have been operating for a relatively short period of time, respectively 12 and 11 years, whereas the Oregon buoy has a 39-year record of wave measurements.

Using the downloaded hourly wave and tide gauge data, we calculated the 2% exceedance elevation of swash maxima, R_2, wave runup using a parameterized equation developed by (Stockdon and others, 2006) (equation 1).

We used a composite beach slope of tan β = 0.064, which reflects a reasonable compromise between the gently sloping sand beach and the steeper gavel beach face. We then combined the calculated hourly wave runup with the measured tides to yield hourly total water levels (TWL), with the resulting levels related to the NAVD88 vertical datum; we converted the measured tides to the NAVD88 datum by subtracting 0.108 m from the hourly values.

$$R_{2\%} = 1.1\left(0.35 \tan\beta \,(H_o L_o)^{\frac{1}{2}} + \frac{[H_o L_o(0.563 \tan\beta^2 + 0.004)]^{\frac{1}{2}}}{2}\right) \quad (1)$$

where tan β is the beach face slope,
H_o is the significant wave height, and
L_o is the deepwater wave length given by $L_o = (g/2\pi)T^2$,
where T is the wave period and g is acceleration due to gravity (9.81 m/s²).

Figure 19 presents the hourly measured significant wave heights (top plot) and calculated total water levels (bottom). Included in the figure are those days when beach surveys were performed, along with the design berm crest elevation of 6.7 m (22 ft). The latter value is important as this is the critical elevation beyond which overtopping and inundation would occur. Also identified is a shaded band that denotes the elevation of the structure toe, above which wave runup is likely to have eroded the structure. This last feature is important for assessing the erosion taking place at the north end of the dynamic revetment.

As can be seen in the top plot of **Figure 19**, the 2013-14 winter produced several major storm wave events, the largest of which occurred on January 12, 2014, in which the significant wave heights reached 9.9 m (32.5 ft). This event remains the largest storm to have affected the structure since its construction. In contrast, other than a few events in late December 2014, the 2014-15 winter the area experienced relatively few storms and generally much lower wave heights. These mild conditions may be better viewed by comparing the wave height anomalies in 2014-15 against a much longer record of waves measured at the Oregon (#46002) wave buoy (**Figure 20**). For the purposes of this comparison we define a long-term mean wave height and subtract the annual seasonal means (e.g., summer/winter) from the long-term value. **Figure 20** shows that the measured waves in 2014-15 are the lowest on record. In contrast, the largest waves occurred in the 1982-83 and 1997-98 winters (**Figure 20**). (The most severe winter on record occurred in 1998-99 (Allan and Komar, 2002b), but the latter event is not included in Figure 20 as the buoy was lost in that particular winter.) Given the generally limited responses to date, this would suggest that the dynamic revetment has yet to be properly tested under elevated wave energy conditions. Because of this, we encourage the USACE to continue to monitor the response of the structure.

The bottom plot of **Figure 19** documents the calculated hourly TWLs for the study site; a 2-hr low-pass loess filter has been fit to the data in order to better highlight the more dominant event signals. As noted previously, the structure was overtopped during a single event on January 12, 2014 (**Figure 14**). Our analyses using the composite beach slope and calculated runup replicates the potential for overtopping of the structure for this storm, along with a second storm that occurred on December 20, 2014. However, this latter event was characterized by much smaller waves and the height of the wave runup was significantly enhanced by the extreme high tides observed at the time. Although we did not visit the site until the end of the 2014-15 winter, we did not see any field evidence remaining on the structure to suggest that it had been overtopped a second time. Of importance, from Figure 20 we can demonstrate that the wave runup during the winter is clearly exceeding the critical toe juncture at the north end leading to its erosion. This process is enhanced by strong wave-wave interaction, the product of waves propagating along the jetty and reflecting off of it where they interact with other incident waves (USACE, 2013).

With the erosion taking place at the north end, gravels are released and slowly transported to the south (**Figure 10** and **Figure 15**). By the end of March 2014 the main mode of gravel was 92 m (301 ft) due south of the northern end of the structure. Interestingly, we identified several discrete cobbles located on the beach in the intertidal zone approximately ~131 m (430 ft) due west of the structure's eroding north end. The cobbles were clearly from the dynamic revetment as they were angular and well weathered, having originated from the core of the gravel berm. Furthermore, several discrete cobbles were found as much as ~430 m (1,410 ft) south of the structure. However, it is unclear if these were transported there by nearshore currents or by some other means. Regardless, at this stage the dominant direction of transport remains to the south. Finally, the gravel mode did not shift significantly in the 2014-2015 period as for much of the time the gravels remained buried beneath the sand.

Figure 19. Wave height and total water level measurements during the study period. Top) Hourly measured significant wave heights determined at the Tillamook (46089) wave buoy located 141 km (88 mi) west of the study site. Bottom) Calculated hourly total water levels (TWLs). Note: vertical dashed lines denote those days when beach surveys were performed, red dashed line denotes the structure crest, and the horizontal shaded region denotes the critical structure toe elevation above which wave runup is likely to erode the structure.

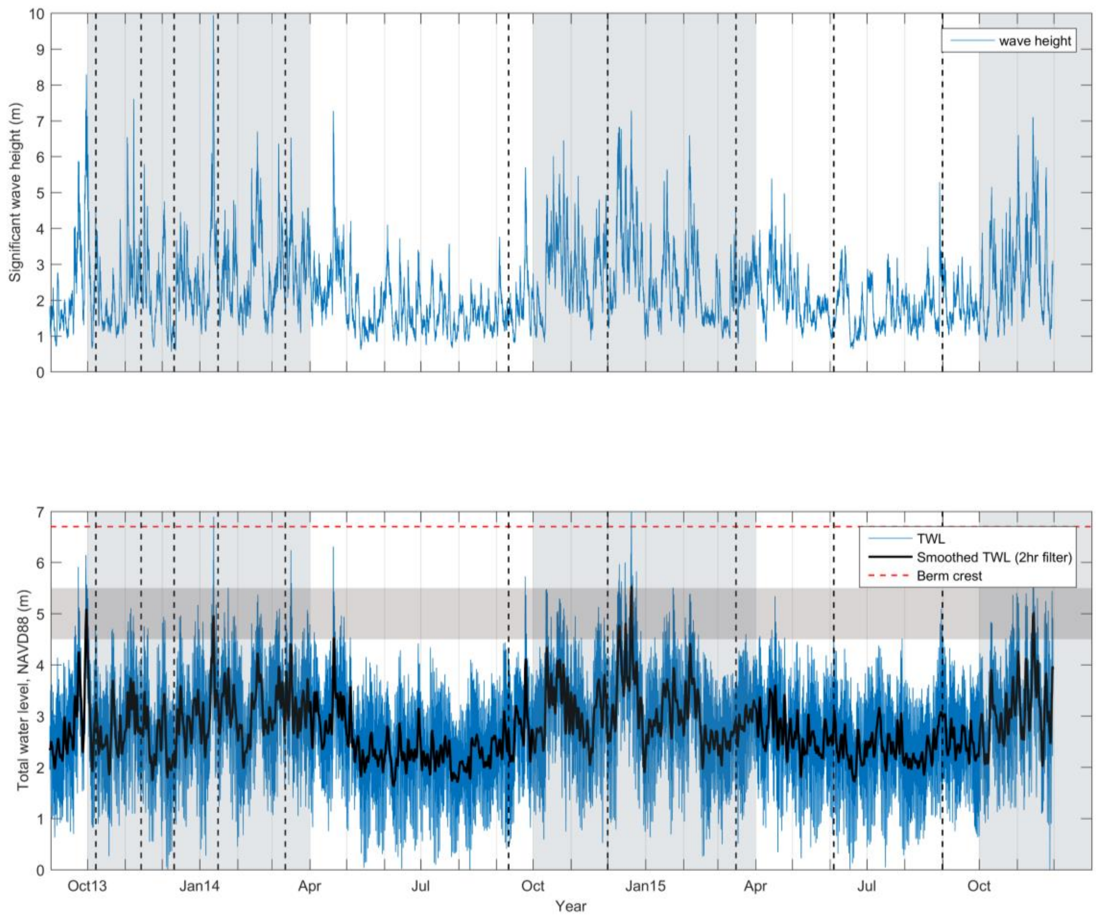

Figure 20. Wave height anomalies calculated for the Oregon (#46002) wave buoy operated by the National Data Buoy Center (NBDC). Anomalies were calculated by determining the long-term mean wave height and subtracting seasonal means from the long-term value. Winter means are calculated for the period January-February-March (JFM), while summer means are based on July-August-September (JAS) conditions.

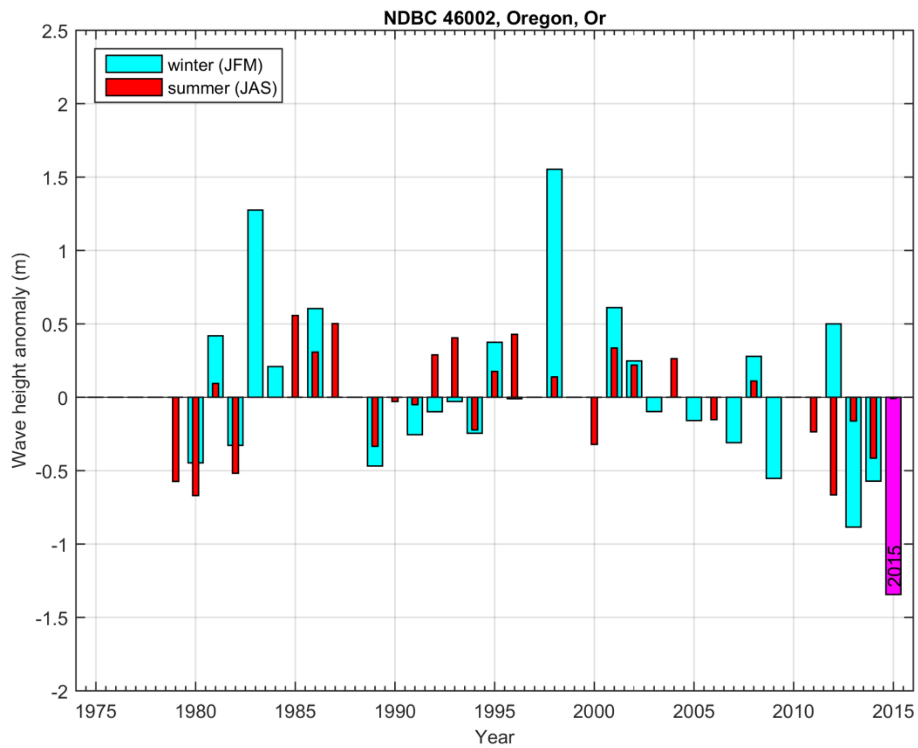

6.0 CONCLUSION

The objective of this report was to describe the initial results from a beach monitoring program established to document the response and efficacy of a dynamic revetment "gravel berm" constructed adjacent to the Columbia River south jetty. The structure was built in order to mitigate an erosion hazard that would almost certainly have led to a breaching of the remaining primary dune located immediately adjacent to the Columbia River south jetty; breaching of the dune could have significant ramifications for the stability of the south jetty and for shoaling at the MCR. The structure was completed in October 2013 and to date has been exposed to almost two years of wave and current processes. This report summarizes the key findings from the monitoring effort.

Dynamic revetments reflect a transitional approach that lies between the construction of "hard" conventional riprap revetment structures formed from boulder size quarry stone, and a beach renourishment project using gravels. Such structures exhibit a remarkable degree of stability in the face of sustained wave attack, a function of the size of the particles (from 4 mm [−2Ø] to 256 mm [−8Ø], including pebbles to large cobbles), and because of their high threshold of motion, requiring strong currents to mobilize the gravels. Furthermore, because of asymmetry in the swash velocities, the gravel size material characteristic of dynamic revetments has a greater propensity for onshore movement, building the beach, as opposed to offshore directed transport typical of sand beaches under sustained wave attack.

Our results to date have documented the following six key responses:

1. The dynamic revetment has experienced significant erosion along its northern distal end (where it abuts against the south jetty). At transect 28, the gravel berm has eroded landward by about 20 m (65.6 ft). The erosion is concentrated along approximately 35–40 m (115–131 ft) of the structure's length. At transect 24, the gravel berm has eroded by 13.7 m (45 ft) since October 2013, and by as much as 15.7 m (51 ft) at transect 25;
2. We estimate that the volume change across the structure amounts to a net loss of ~2,300 m^3 (3,000 yd^3) of material to date. All of this loss can be attributed to erosion taking place at the north end of the gravel berm;
3. Gravels eroded from the structure are being transported to the south. As of March 2014, the primary gravel mode was located some 92 m (301 ft) due south of the northern end of the structure. This mode of gravel did not shift significantly in the 2014-15 period as for much of the time the gravel was buried beneath the sand;
4. To date, the structure has withstood at least two major wave events with at least one of these resulting in minor overtopping of the south central portion of the gravel berm. Erosion of the structure was highest in the initial 2013-14 winter, a function of generally higher wave energy levels and higher wave runup, and slowed over the 2014-15 winter due to the absence of significant storms;
5. Along much of the structure's length, sand is accumulating on the structure crest, and against the juncture of the gravel berm and dune line; and
6. Our analyses have highlighted the occurrence of more energetic winters in past years, characterized by much larger wave heights (and potentially greater wave runup), when compared with recent winters. As a result, the Columbia River dynamic revetment remains to be fully tested under these more dynamic wave energy conditions.

7.0 ACKNOWLEDGMENTS

Funding for this study was provided by the U.S. Army Corps of Engineers, Portland District under grant award W9127N-13-2-0002-0002. We are grateful to Mr. Rod Moritz for his technical advice throughout this project. We would especially like to acknowledge Dr. Paul Komar for his review of the report.

8.0 REFERENCES

Ahrens, J.P., 1990, Dynamic revetments, *in* Proceedings of 22nd Conference on Coastal Engineering, Delft, The Netherlands, 1990: Reston, Va., American Society of Civil Engineers, p. 1837–1850.

Allan, J.C., and Hart, R., 2007a, Profile dynamics and particle tracer mobility of a cobble berm constructed on the Oregon coast, *in* Coastal Sediments' 07, Coastal Engineering and Science in Cascading Spatial and Temporal Scales, New Orleans, La., Proceedings: p. 449–462.

Allan, J.C., and Hart, R., 2007b, Assessing the temporal and spatial variability of coastal change in the Neskowin littoral cell: Developing a comprehensive monitoring program for Oregon beaches: Oregon Department of Geology and Mineral Industries Open-File Report O-07-01, 27 p.

Allan, J.C., and Hart, R., 2008, Oregon beach and shoreline mapping and analysis program: 2007-2008 beach monitoring report: Oregon Department of Geology and Mineral Industries Open-File Report O-08-15, 60 p.

Allan, J.C., and Komar, P.D., 2002a, A dynamic revetment and artificial dune for shore protection, *in* Proceedings of 28th Conference on Coastal Engineering, Wales, United Kingdom, 2002: Reston, Va., American Society of Civil Engineers, p. 2044–2056.

Allan, J.C., and Komar, P.D., 2002b, Extreme storms on the Pacific Northwest Coast during the 1997-98 El Niño and 1998-99 La Niña: Journal of Coastal Research, v. 18, no. 1, p. 175–193.

Allan, J.C., and Komar, P.D., 2004, Environmentally compatible cobble berm and artificial dune for shore protection: Shore & Beach, v. 72, no. 1, p. 9–18.

Allan, J.C., Hart, R., and Geitgey, R., 2005, Dynamic revetments for coastal erosion stabilization: A feasibility analysis for application on the Oregon Coast: Oregon Department of Geology and Mineral Industries Special Paper 37, 71 p.

Allan, J.C., Hart, R., and Tranquilli, V., 2006, The use of Passive Integrated Transponder tags (PIT-tags) to trace cobble transport in a mixed sand-and-gravel beach on the high-energy Oregon coast, USA: Marine Geology, v. 232, no. 1-2, p. 63–86.

Allan, J.C., Ruggiero, P., Garcia, G., Harris, E.L., Roberts, J. T., and Stimely, L., 2015a, Coastal flood hazard study, Clatsop County, Oregon: Oregon Department of Geology and Mineral Industries Open-File Report O-15-05, 202 p.

Allan, J.C., Ruggiero, P., Garcia, G., O'Brien, F., Stimely, L., and Roberts, J.T., 2015b, Coastal flood hazard study, Tillamook County, Oregon: Oregon Department of Geology and Mineral Industries Special Paper 47, 283 p.

Bernstein, D.J., Freeman, C., Forte, M.F., Park, J.-Y., Gayes, P.T., and Mitasova, H., 2003, Survey design analysis for three-dimensional mapping of beach and nearshore morphology, *in* Coastal Sediments '03, Clearwater Beach, Fla.: Reston, Va., American Society of Civil Engineers, p. 12.

Bird, E., and Lewis, N., 2015, Beach renourishment: New York, Springer, 137 p.

Bradbury, A.P., and Powell, K.A., 1992, The short term response of shingle spits to storm wave action: Coastal Engineering, v. 16, p. 2695–2707.

Bruun, P., and Johannesson, P., 1976, Parameters affecting stability of rubble mounds: Journal of Waterways, Harbors and Coastal Engineering Division, v. 102, no. 2, 141-164.

Cooper, W.S., 1958, Coastal sand dunes of Oregon and Washington: Boulder, Colo., Geological Society of America. Memoir 72, p. 169.

Dornbusch, U., Williams, R.B.G., Moses, C., and Robinson, D.A., 2002, Life expectancy of shingle beaches: measuring in situ abrasion: Journal of Coastal Research, v. 36, Special Issue, p. 249–255.

Downie, K.A., and Saaltink, H., 1983, An artificial cobble beach for erosion control, *in* Coastal Structures '83: Reston, Va., American Society of Civil Engineers, p. 846–859.

Everts, C.H., Eldon, C.D., and Moore, J., 2002, Performance of cobble berms in Southern California: Shore & Beach, v. 70, no. 4, p. 5–14.

Gelfenbaum, G., Buijsman, M.C., Sherwood, C.R., Moritz, H.R., and Gibbs, A.E., 2001, Coastal evolution and sediment budget at the mouth of the Columbia River, USA, *in* Proceedings of the 4th International Conference on Coastal Dynamics, Lund, Sweden: Reston, Va., American Society of Civil Engineers, p. 818–827.

Horn, D.P., 1992, A numerical model for shore-normal sediment size variation on a macrotidal beach: Earth Surface Processes and Landforms, v. 17, p. 755–773.

Inman, D.L., 1949, Sorting of sediments in the light of fluid mechanics: Journal of Sedimentary Petrology, v. 19, no. 2, p. 51–70.

Johnson, C.N., 1987, Rubble beaches versus revetments, *in* Coastal Sediments '87, New Orleans, La., Proceedings: Reston, Va., American Society of Civil Engineers, p. 1217–1231.

Kirk, R.M., 1992, Experimental beach reconstruction-renourishment on mixed sand and gravel beaches, Washdyke Lagoon, South Canterbury, New Zealand: Coastal Engineering, v. 17, p. 253–277.

Komar, P.D., Allan, J.C., and Winz, R., 2003, Cobble beaches—The "design with nature" approach for shore protection, *in* Coastal Sediments' 03, Clearwater Beach, Fla.: Reston, Va., American Society of Civil Engineers.

Lockett, J.B., 1963, Phenomena affecting improvement of the lower Columbia estuary and entrance, *in* Federal Interagency Sedimentation Conference, Jackson, Mississippi: Washington, D.C., U.S. Department of Agriculture, Miscellaneous Publication 970, p. 626–668.

Loman, G.J.A., Van Gent, M.R.A., and Markvoort, J.W., 2010, Physical model testing of an innovative cobble shore, Part 1: verification of cross-shore profile deformation, *in* Coastlab 10: Proceedings on the Third International Conference on the Application of Physical Modelling to Port and Coastal Protection, Sept. 28th-30th & October 1st, 2010, Barcelona, Spain: International Centre for Coastal Resources.

Lorang, M.S., 1991, An artificial perch-gravel beach as a shore protection structure, *in* Coastal Sediments 91, Seattle, Washington, Proceedings, vol. 2: Reston, Va., American Society of Civil Engineers American Society of Civil Engineers, p. 1916–1925.

Morton, R.A., Leach, M.P., Paine, J.G., and Cardoza, M.A., 1993, Monitoring beach changes using GPS surveying techniques: Journal of Coastal Research, v. 9, no. 3, p. 702–720.

Muir Wood, A.M., 1970, Characteristics of shingle beaches: The solution to some practical problems, *in* Proceedings of 12th Conference on Coastal Engineering, Washington, D.C., 1970: Reston, Va., American Society of Civil Engineers, p. 1059–1075.

Nicholls, R., and Webber, N., 1988, Characteristics of shingle beaches with reference to Christchurch Bay, S. England, *in* Proceedings of the 21st Conference on Coastal Engineering, Torremolinos, Spain, 1988: Reston, Va., American Society of Civil Engineers.

Ruggiero, P., and Voigt, B., 2000, Beach monitoring in the Columbia River littoral cell, 1997–2000: Coastal Monitoring & Analysis Program, Washington Department of Ecology Publication No. 00-06-026, 113 p.

Ruggiero, P., Kaminsky, G.M., Gelfenbaum, G., and Voight, B., 2005, Seasonal to interannual morphodynamics along a high-energy dissipative littoral cell: Journal of Coastal Research, v. 21, no. 3, p. 553–578.

Sherman, D.J., 1991, Gravel beaches: National Geographic Research and Exploration, v. 7, no. 4, p. 442–452.

Sherwood, C.R., Jay, D.A., Harvey, R.B., Hamilton, P., and Simenstad, C.A., 1990, Historical changes in the Columbia River Estuary: Progress in Oceanography, v. 25, p. 299–352.

Stockdon, H.F., Holman, R.A., Howd, P.A., and Sallenger, A.H., 2006, Empirical parameterization of setup, swash, and runup: Coastal Engineering, v. 53, no. 7, p. 573–588.

Trimble, 2005, Trimble 5700 GPS system datasheet: Trimble Navigation Limited, 2 p.

USACE, 2013, Mouth of the Columbia River south jetty dune stabilization, Fort Stevens, Oregon: U.S. Army Corps of Engineers, Design Documentation Report, final draft, Feb. 25, 2013, 100 p.

Van der Werf, I., and Van Gent, M.R.A., 2010, Gravel beaches with seawalls, *in* Proceedings of 32nd Conference on Coastal Engineering, Shanghai, China, 2010: Reston, Va., American Society of Civil Engineers, p. 1853–1867.

van Hijum, E., 1974, Equilibrium profiles of coarse material under wave attack, *in* Proceedings of 14th Conference on Coastal Engineering, Copenhagen, Denmark, 1974: Reston, Va., American Society of Civil Engineers, p. 939–957.

Ward, D.L., and Ahrens, J.P., 1991, Laboratory study of a dynamic berm revetment: Vicksburg, Miss., U.S. Army Corps of Engineers, Coastal Engineering Research Center, Waterways Experiment Station, Technical report CERC-92-1, 78 p..

Willis, D.H., Baird, W.F., and Magoon, O.T., 1988, Berm breakwaters: New York, American Society of Civil Engineers, 284 p.

Woxell, L.K., 1998, Prehistoric beach accretion rates and long-term response to sediment depletion in the Columbia River littoral system, USA: Portland, Oreg., Portland State University, M.S. thesis, 206 p.

Zenkovich, V.P., 1967, Processes of coastal development, Eng. lang. ed., J.A. Steers: Edinburgh, Oliver and Boyd.

9.0 APPENDIX: COLUMBIA RIVER SOUTH JETTY DYNAMIC REVETMENT PROFILES

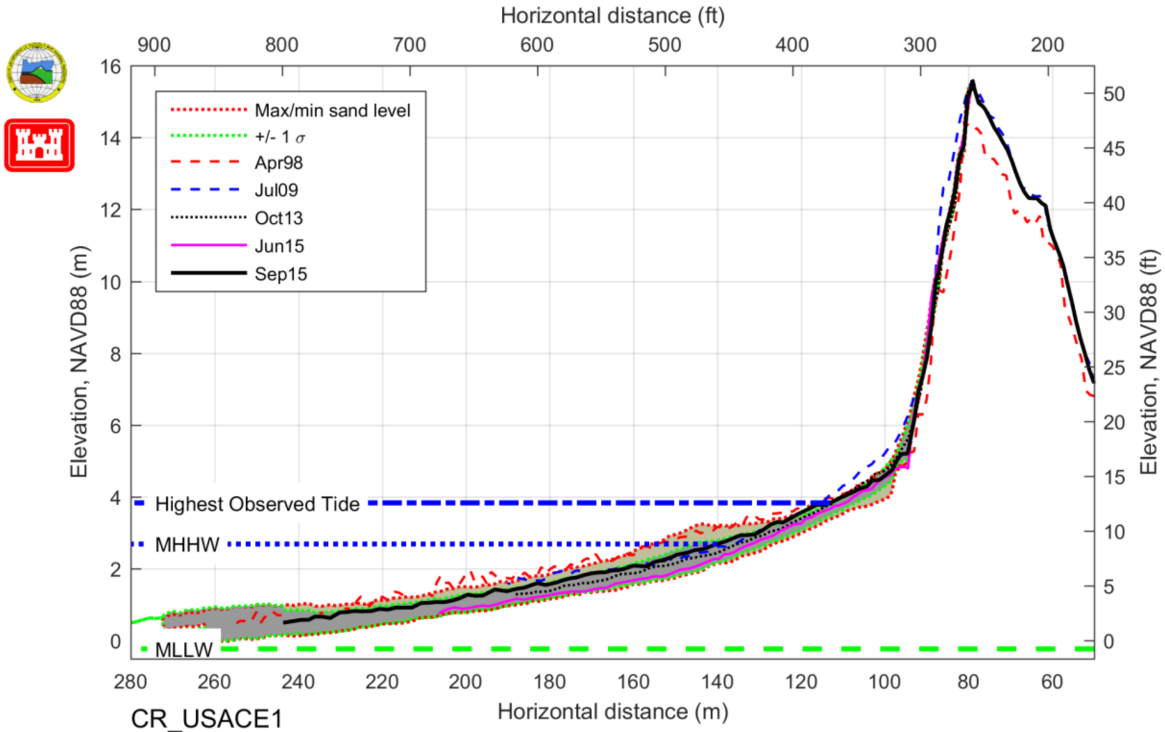

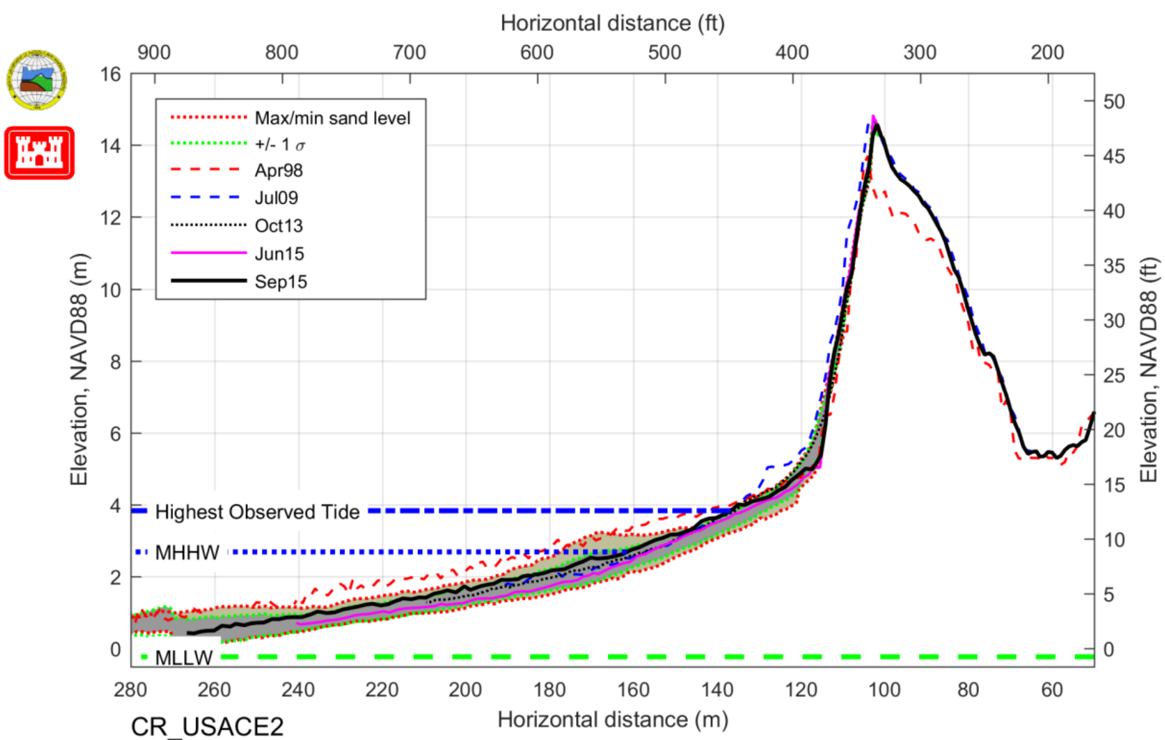

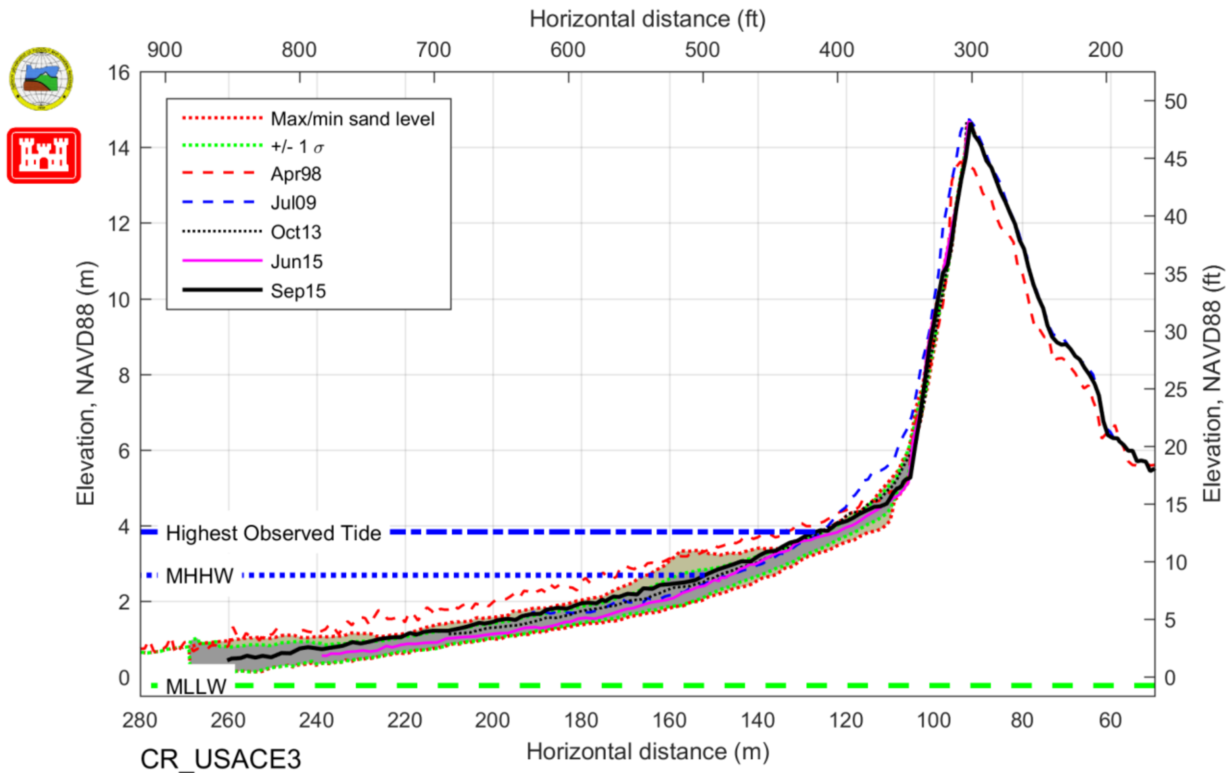
Horizontal distance (ft)
Max/min sand level
+/- 1 σ
Apr98
Jul09
Oct13
Jun15
Sep15
Highest Observed Tide
MHHW
MLLW
Elevation, NAVD88 (m)
Elevation, NAVD88 (ft)
Horizontal distance (m)
CR_USACE3

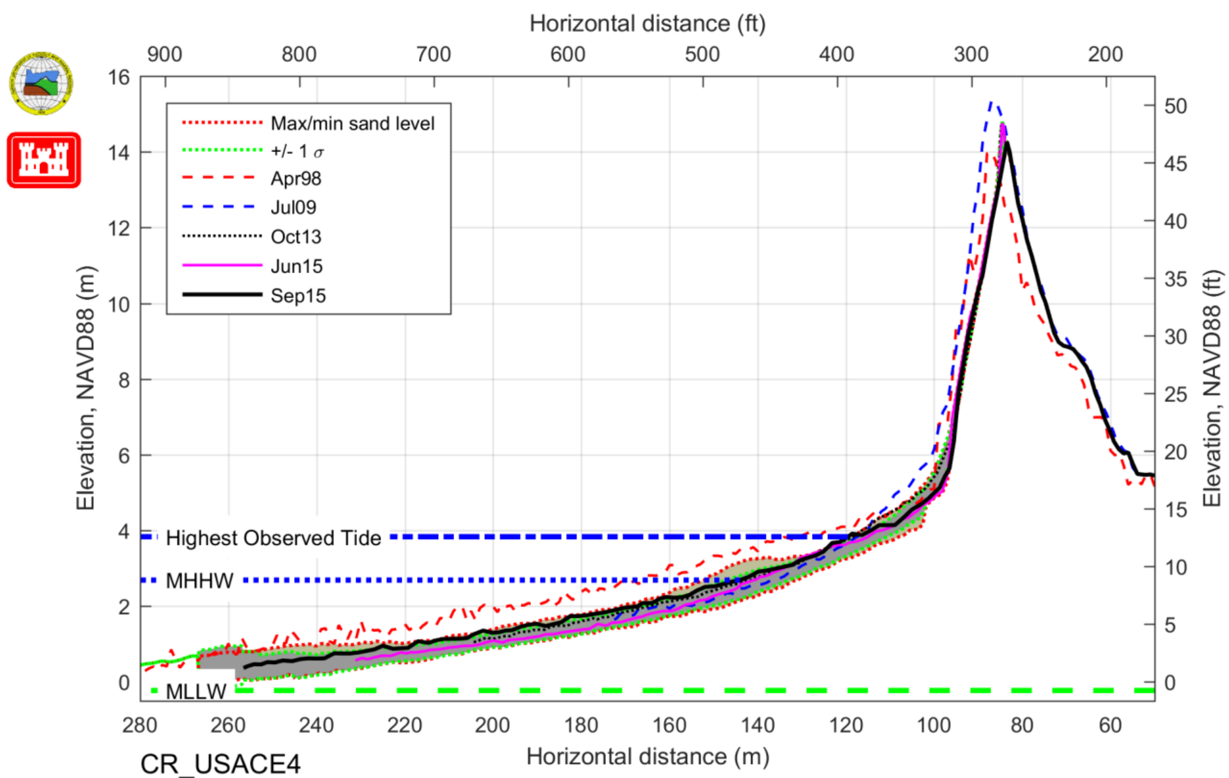
Horizontal distance (ft)
Max/min sand level
+/- 1 σ
Apr98
Jul09
Oct13
Jun15
Sep15
Highest Observed Tide
MHHW
MLLW
Elevation, NAVD88 (m)
Elevation, NAVD88 (ft)
Horizontal distance (m)
CR_USACE4

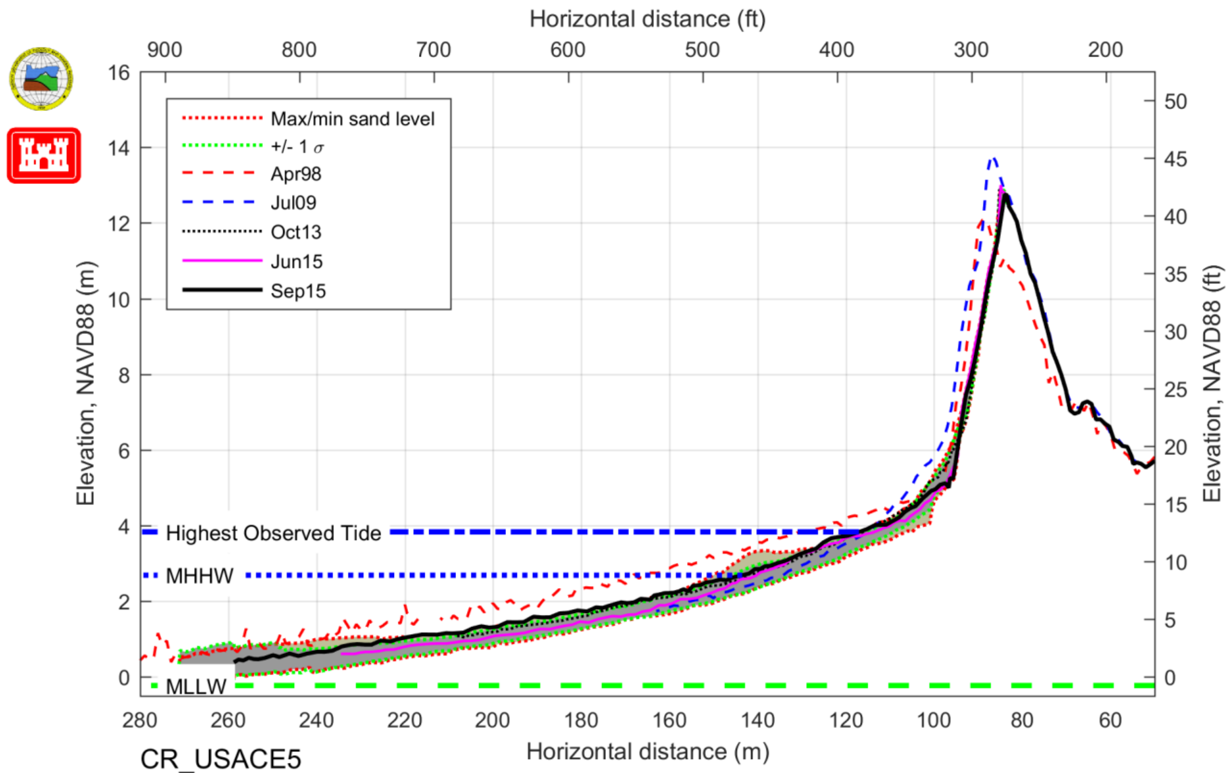
Horizontal distance (ft)
Max/min sand level
+/- 1 σ
Apr98
Jul09
Oct13
Jun15
Sep15
Highest Observed Tide
MHHW
MLLW
Elevation, NAVD88 (m)
Elevation, NAVD88 (ft)
Horizontal distance (m)
CR_USACE5

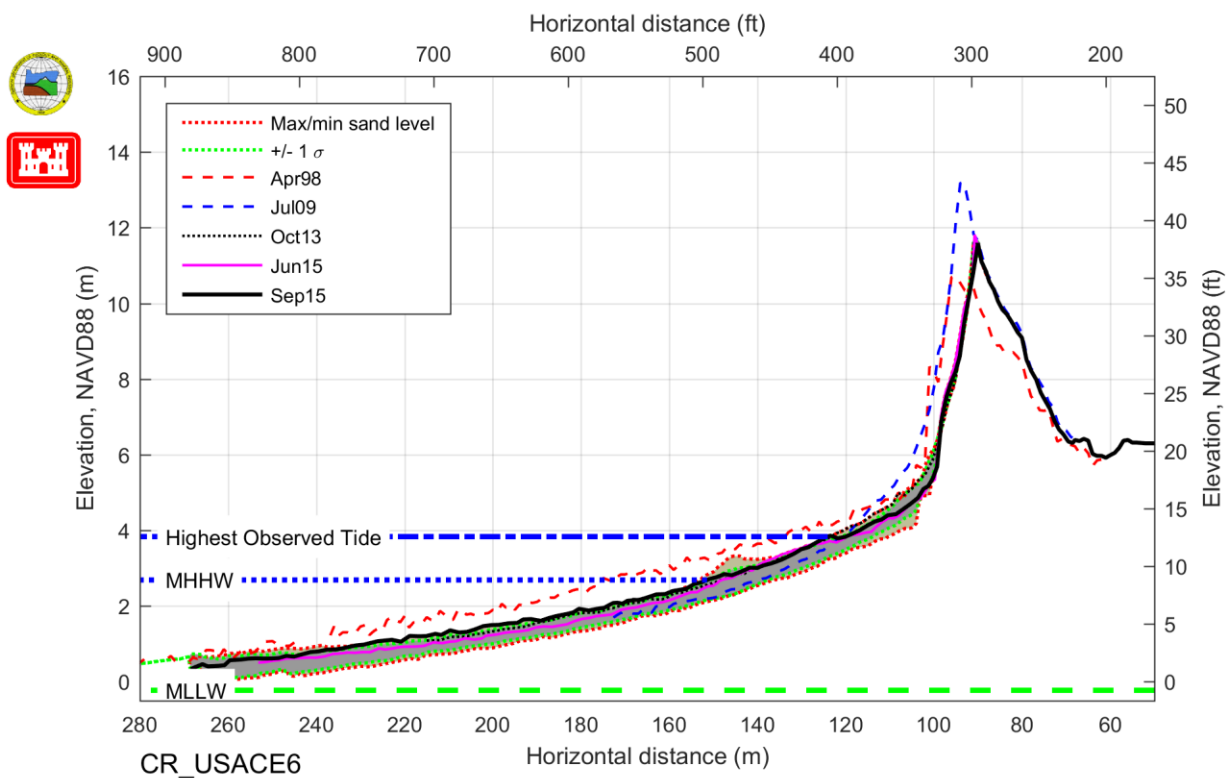
Horizontal distance (ft)
Max/min sand level
+/- 1 σ
Apr98
Jul09
Oct13
Jun15
Sep15
Highest Observed Tide
MHHW
MLLW
Elevation, NAVD88 (m)
Elevation, NAVD88 (ft)
Horizontal distance (m)
CR_USACE6

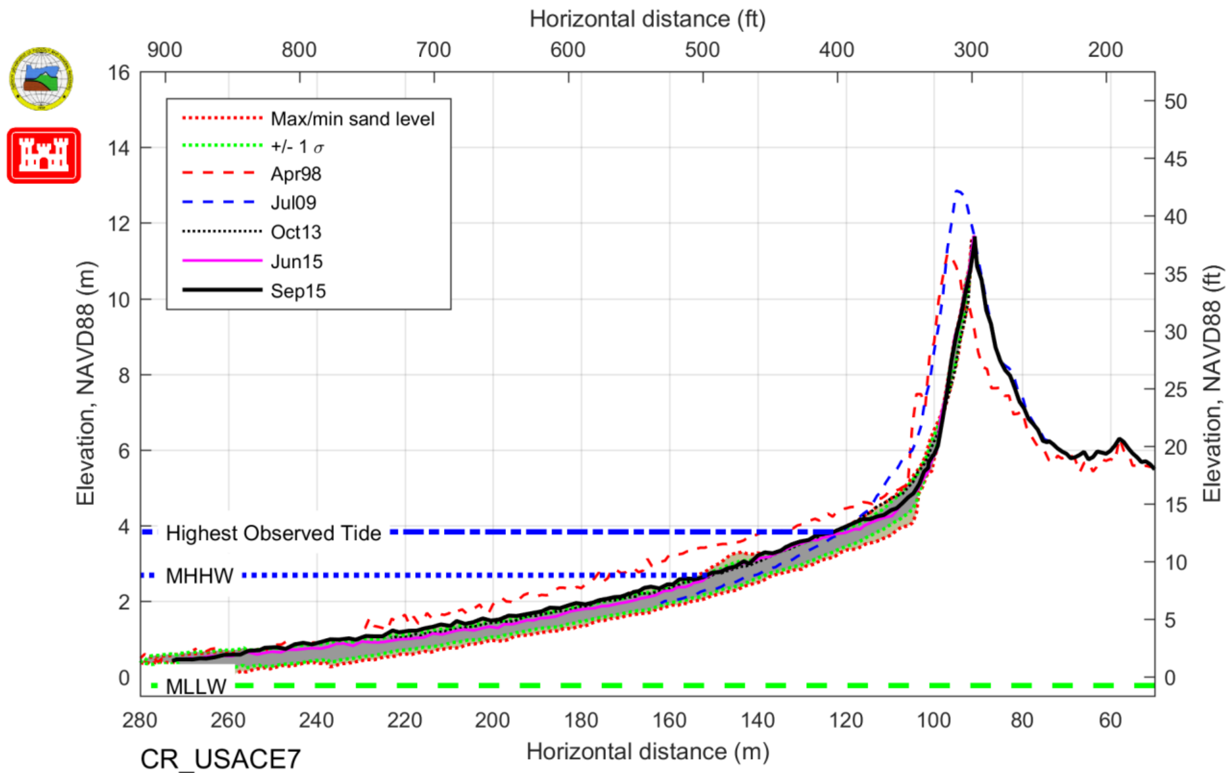
Horizontal distance (ft)
900
800
700
600
500
400
300
200
Max/min sand level
+/- 1 σ
Apr98
Jul09
Oct13
Jun15
Sep15
Highest Observed Tide
MHHW
MLLW
Elevation, NAVD88 (m)
Elevation, NAVD88 (ft)
16
14
12
10
8
6
4
2
0
50
45
40
35
30
25
20
15
10
5
0
280
260
240
220
200
180
160
140
120
100
80
60
Horizontal distance (m)
CR_USACE7

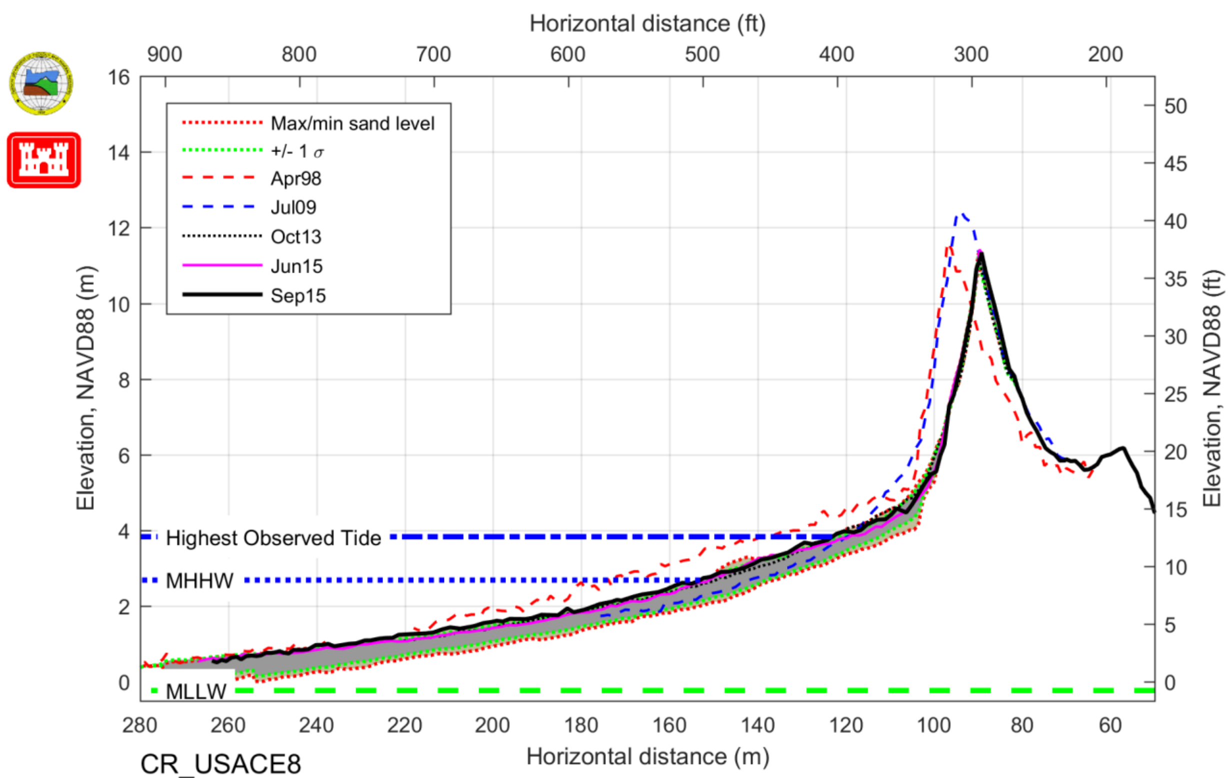
Horizontal distance (ft)
900
800
700
600
500
400
300
200
Max/min sand level
+/- 1 σ
Apr98
Jul09
Oct13
Jun15
Sep15
Highest Observed Tide
MHHW
MLLW
Elevation, NAVD88 (m)
Elevation, NAVD88 (ft)
16
14
12
10
8
6
4
2
0
50
45
40
35
30
25
20
15
10
5
0
280
260
240
220
200
180
160
140
120
100
80
60
Horizontal distance (m)
CR_USACE8

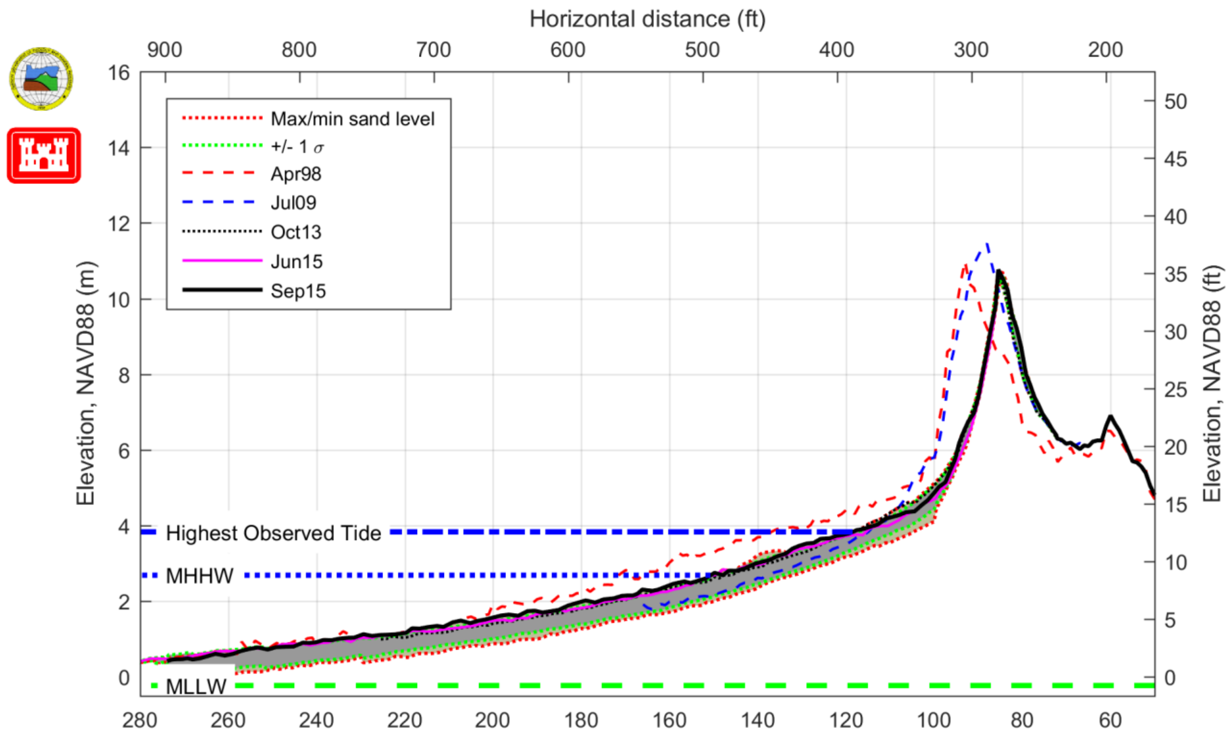

CR_USACE9

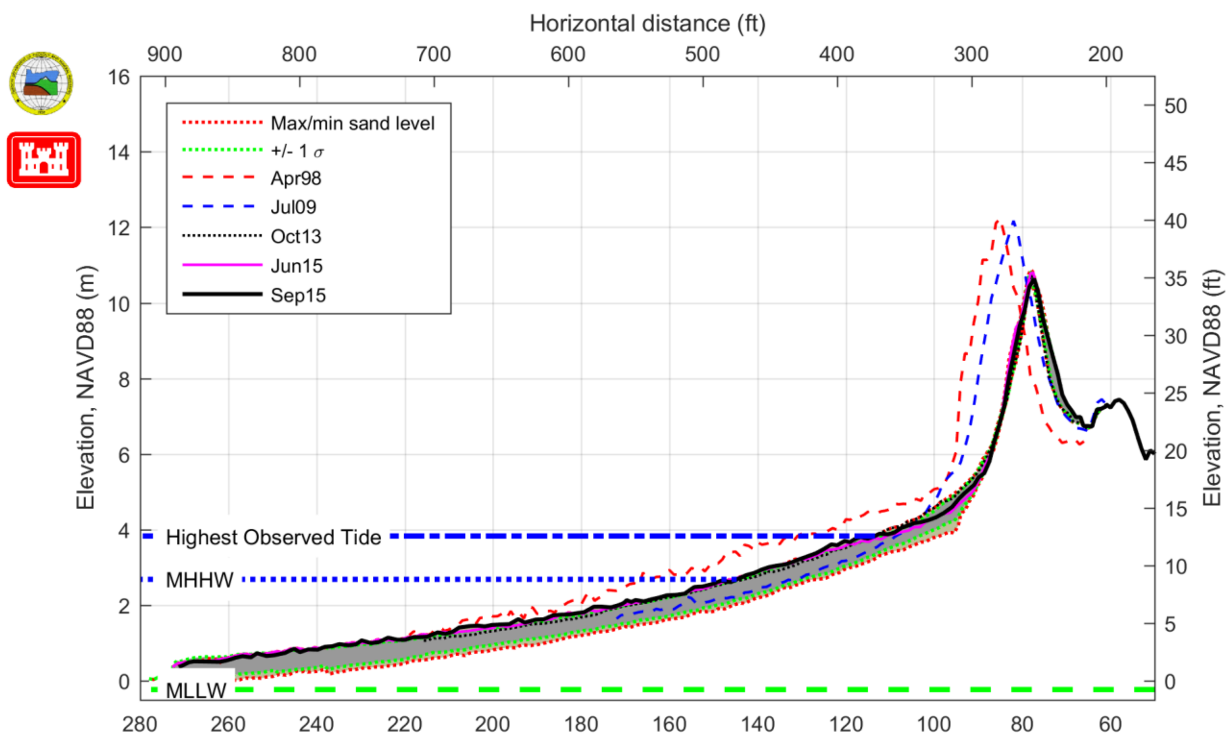

CR_USACE10

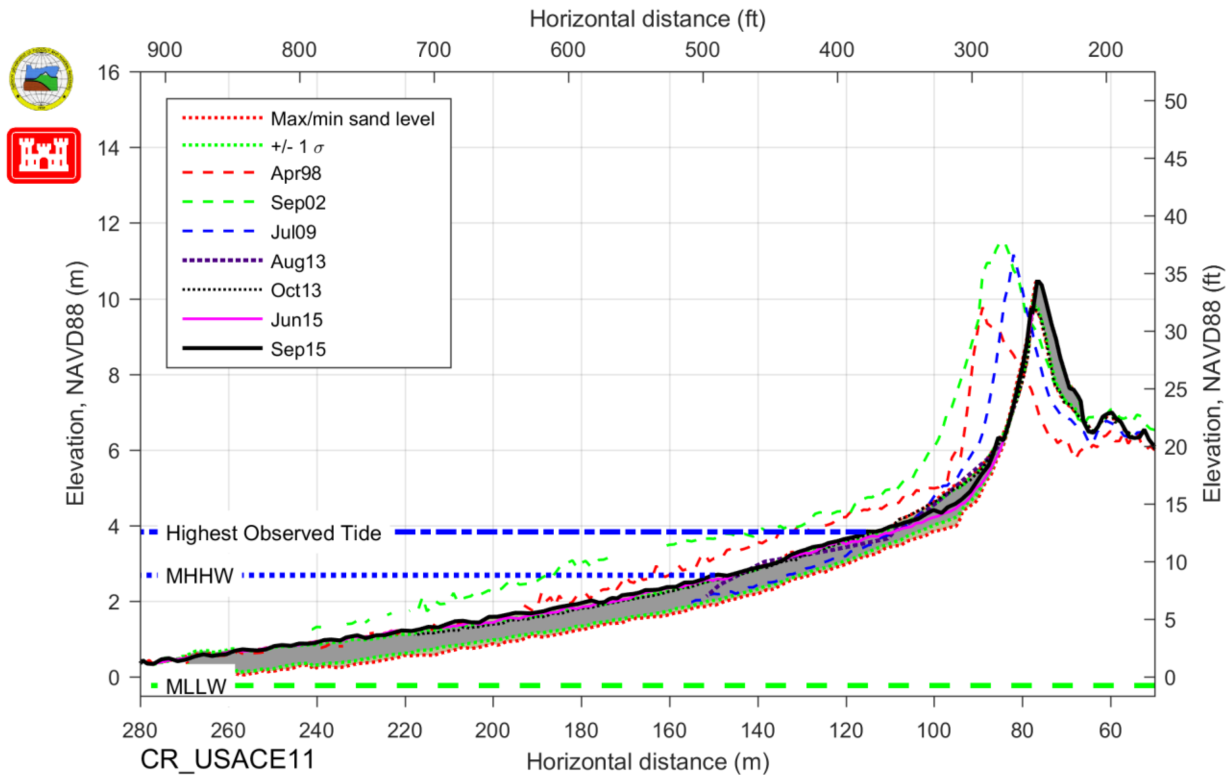
Horizontal distance (ft)
900 800 700 600 500 400 300 200
Max/min sand level
+/- 1 σ
Apr98
Sep02
Jul09
Aug13
Oct13
Jun15
Sep15
Highest Observed Tide
MHHW
MLLW
Elevation, NAVD88 (m)
Elevation, NAVD88 (ft)
280 260 240 220 200 180 160 140 120 100 80 60
Horizontal distance (m)
CR_USACE11

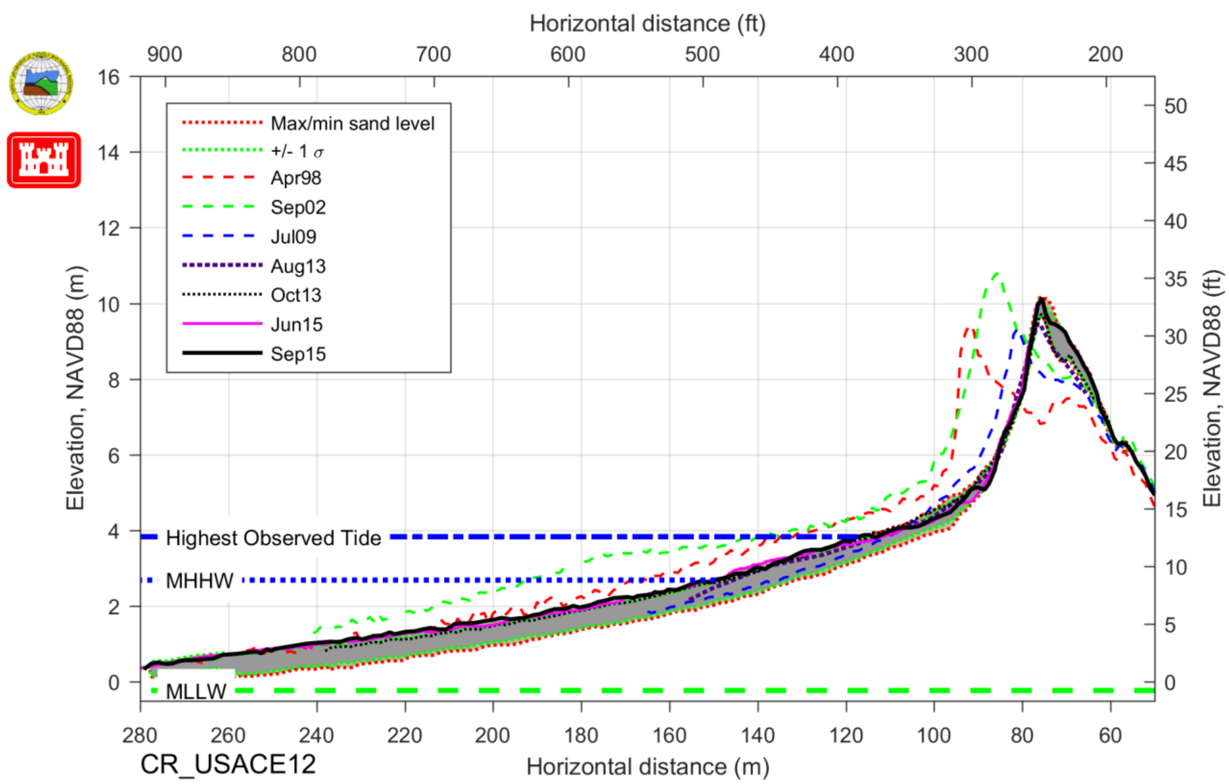
Horizontal distance (ft)
900 800 700 600 500 400 300 200
Max/min sand level
+/- 1 σ
Apr98
Sep02
Jul09
Aug13
Oct13
Jun15
Sep15
Highest Observed Tide
MHHW
MLLW
Elevation, NAVD88 (m)
Elevation, NAVD88 (ft)
280 260 240 220 200 180 160 140 120 100 80 60
Horizontal distance (m)
CR_USACE12

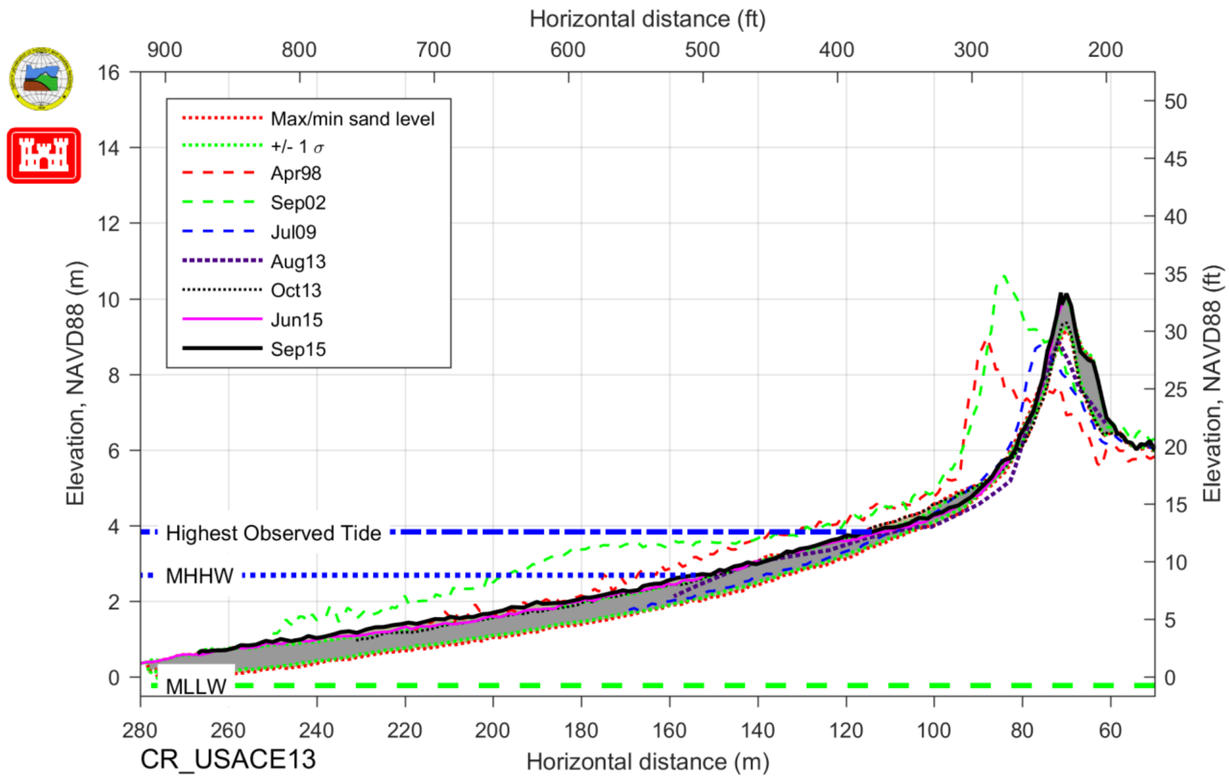
Horizontal distance (ft)
Elevation, NAVD88 (m)
Elevation, NAVD88 (ft)
Max/min sand level
+/- 1 σ
Apr98
Sep02
Jul09
Aug13
Oct13
Jun15
Sep15
Highest Observed Tide
MHHW
MLLW
CR_USACE13
Horizontal distance (m)

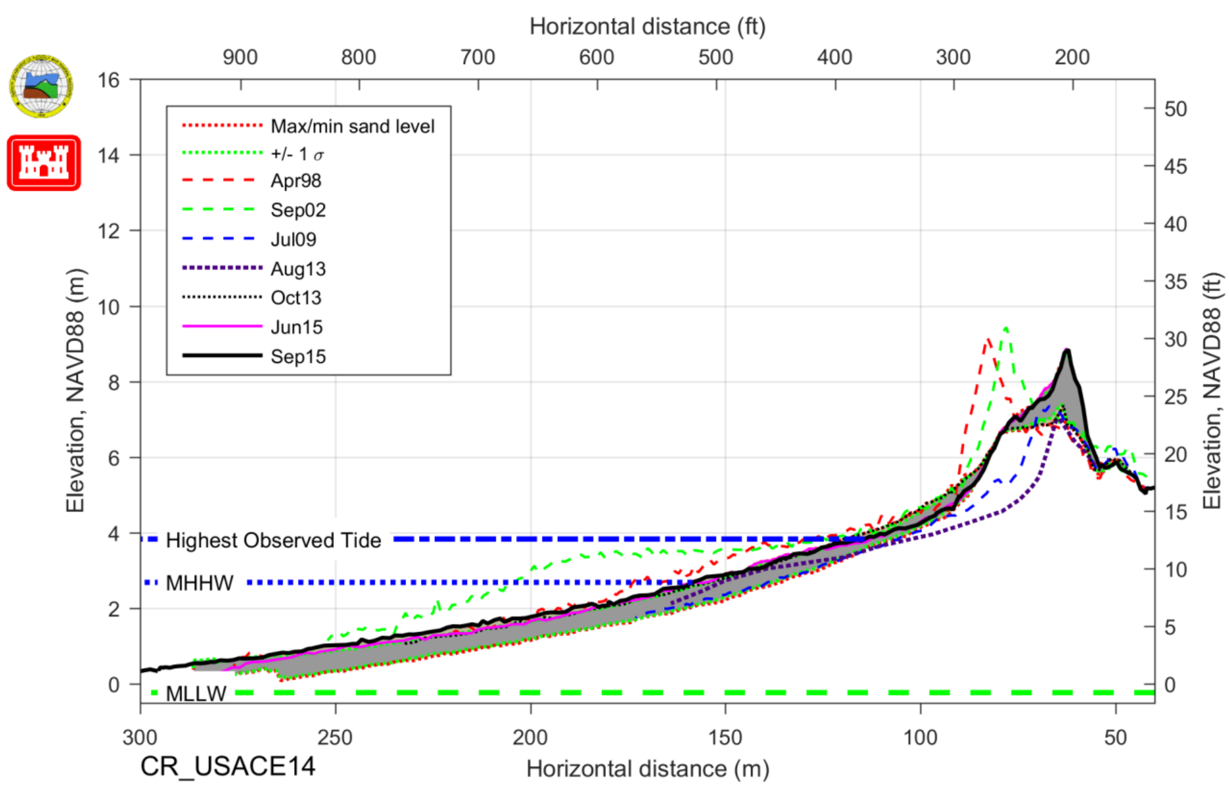
Horizontal distance (ft)
Elevation, NAVD88 (m)
Elevation, NAVD88 (ft)
Max/min sand level
+/- 1 σ
Apr98
Sep02
Jul09
Aug13
Oct13
Jun15
Sep15
Highest Observed Tide
MHHW
MLLW
CR_USACE14
Horizontal distance (m)

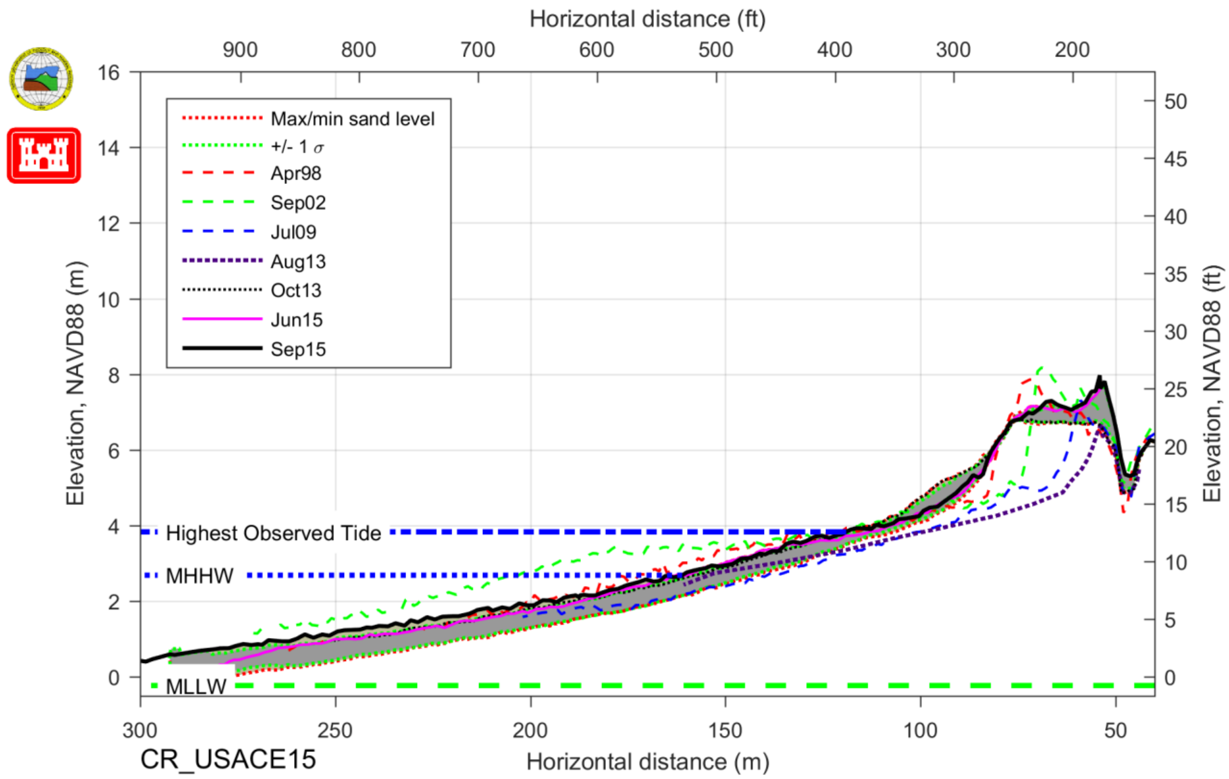
Horizontal distance (ft)
900
800
700
600
500
400
300
200
Max/min sand level
+/- 1 σ
Apr98
Sep02
Jul09
Aug13
Oct13
Jun15
Sep15
Elevation, NAVD88 (m)
Elevation, NAVD88 (ft)
Highest Observed Tide
MHHW
MLLW
Horizontal distance (m)
CR_USACE15

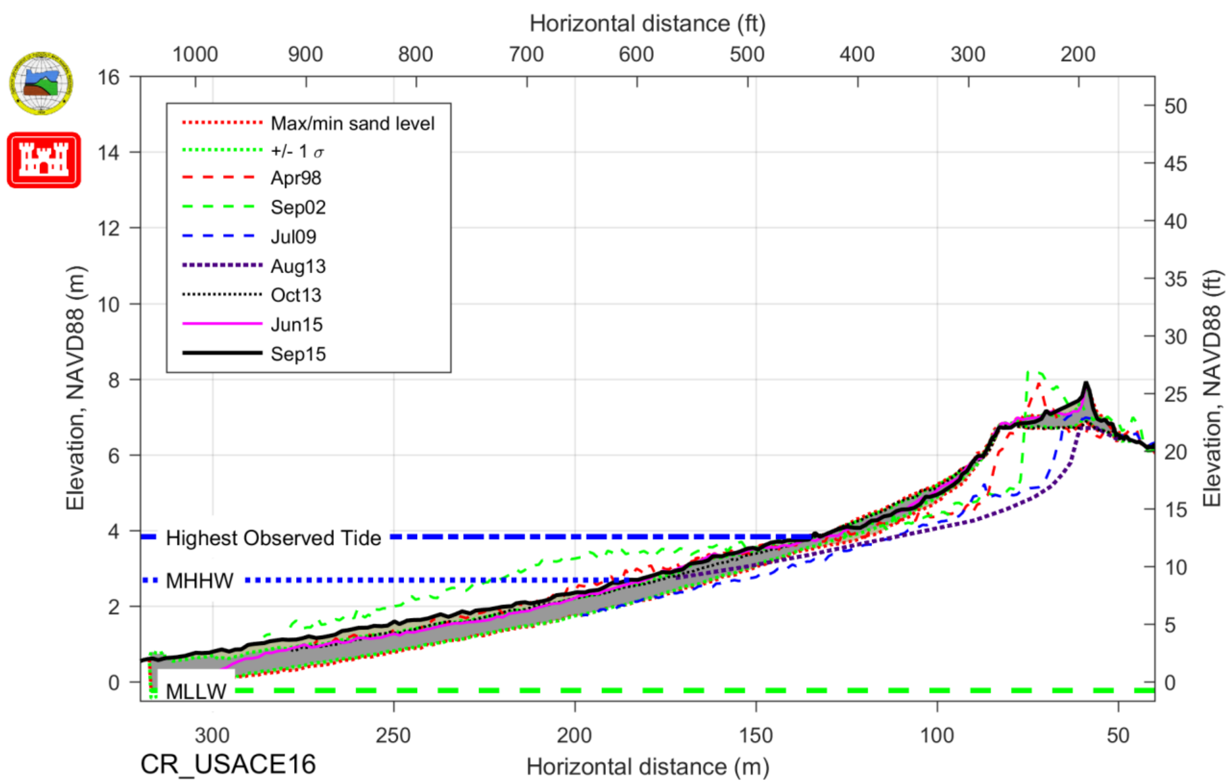
Horizontal distance (ft)
1000
900
800
700
600
500
400
300
200
Max/min sand level
+/- 1 σ
Apr98
Sep02
Jul09
Aug13
Oct13
Jun15
Sep15
Elevation, NAVD88 (m)
Elevation, NAVD88 (ft)
Highest Observed Tide
MHHW
MLLW
Horizontal distance (m)
CR_USACE16

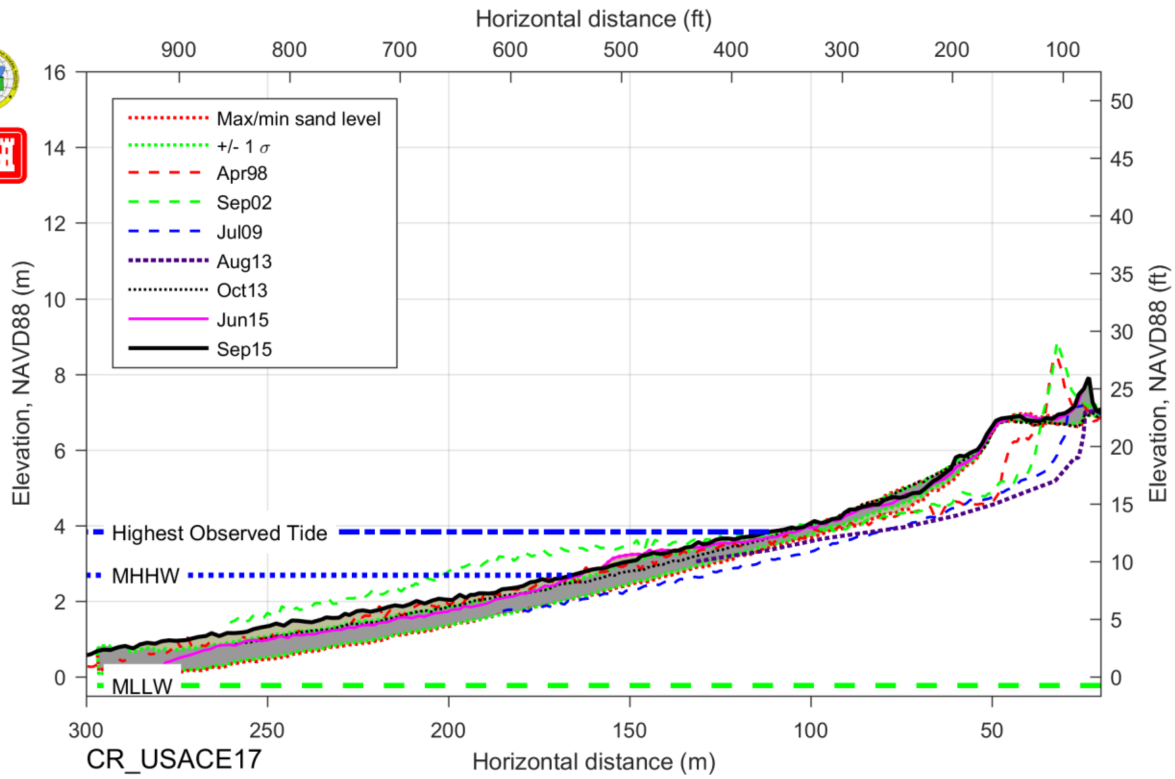
Horizontal distance (ft)
Max/min sand level
+/- 1 σ
Apr98
Sep02
Jul09
Aug13
Oct13
Jun15
Sep15
Highest Observed Tide
MHHW
MLLW
Elevation, NAVD88 (m)
Elevation, NAVD88 (ft)
CR_USACE17
Horizontal distance (m)

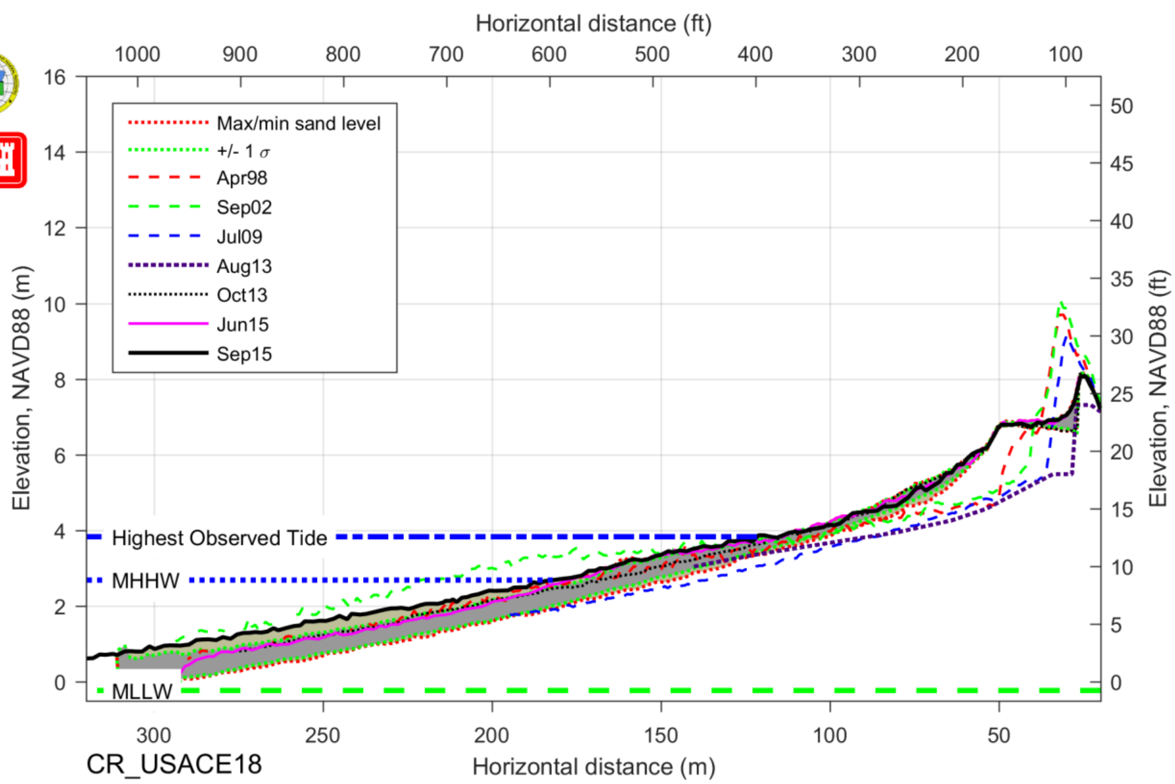
Horizontal distance (ft)
Max/min sand level
+/- 1 σ
Apr98
Sep02
Jul09
Aug13
Oct13
Jun15
Sep15
Highest Observed Tide
MHHW
MLLW
Elevation, NAVD88 (m)
Elevation, NAVD88 (ft)
CR_USACE18
Horizontal distance (m)

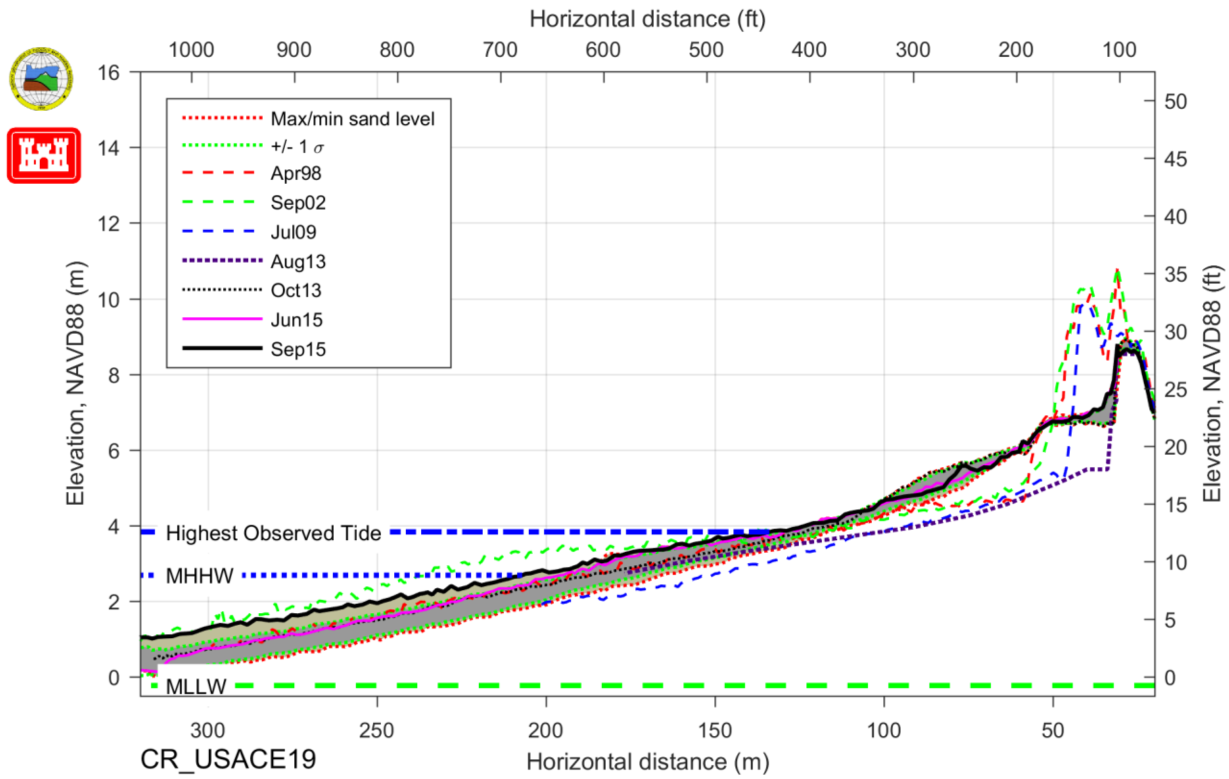
Horizontal distance (ft)
Elevation, NAVD88 (m)
Elevation, NAVD88 (ft)
Max/min sand level
+/- 1 σ
Apr98
Sep02
Jul09
Aug13
Oct13
Jun15
Sep15
Highest Observed Tide
MHHW
MLLW
CR_USACE19
Horizontal distance (m)

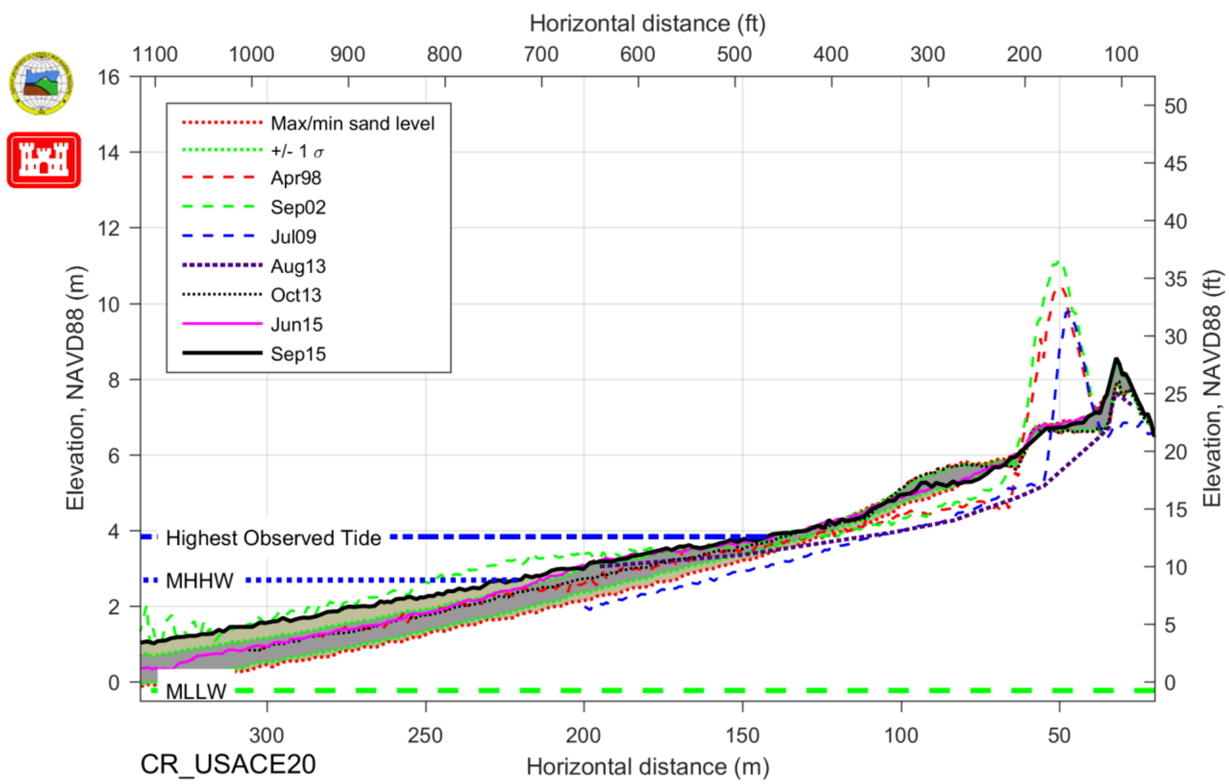
Horizontal distance (ft)
Elevation, NAVD88 (m)
Elevation, NAVD88 (ft)
Max/min sand level
+/- 1 σ
Apr98
Sep02
Jul09
Aug13
Oct13
Jun15
Sep15
Highest Observed Tide
MHHW
MLLW
CR_USACE20
Horizontal distance (m)

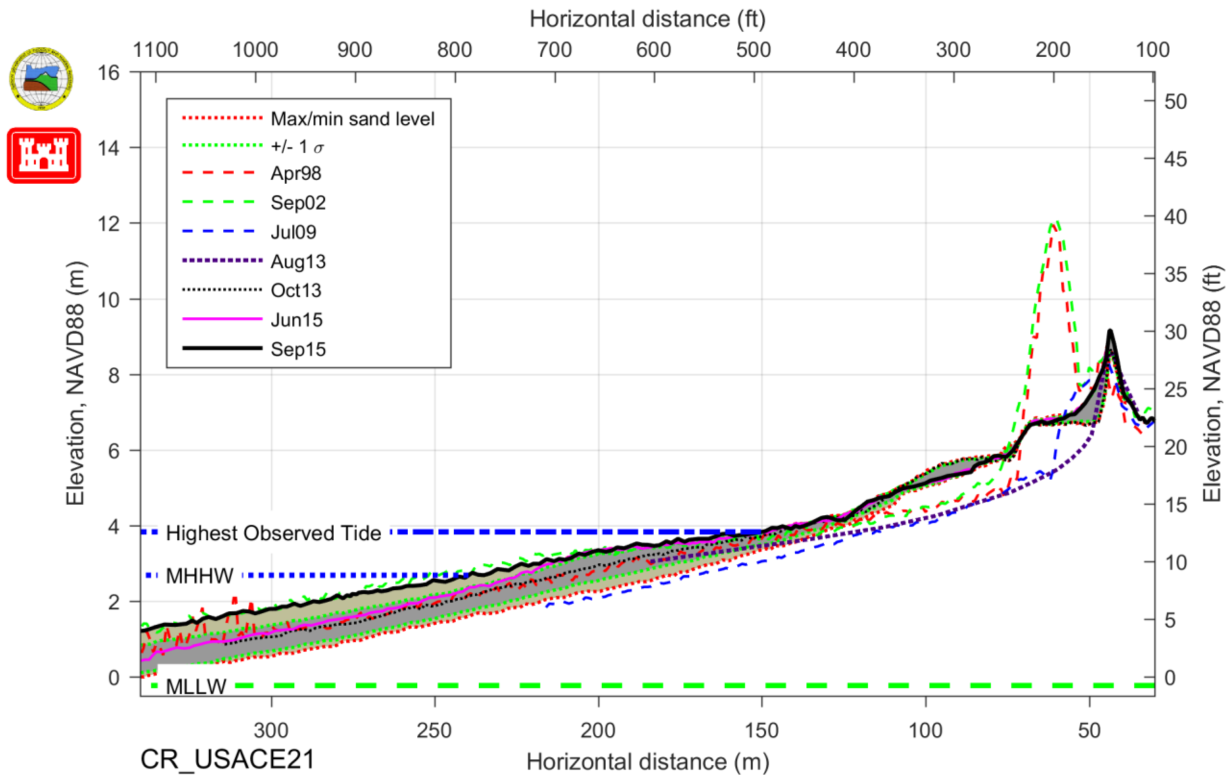
Horizontal distance (ft)
Max/min sand level
+/- 1 σ
Apr98
Sep02
Jul09
Aug13
Oct13
Jun15
Sep15
Highest Observed Tide
MHHW
MLLW
Elevation, NAVD88 (m)
Elevation, NAVD88 (ft)
Horizontal distance (m)
CR_USACE21

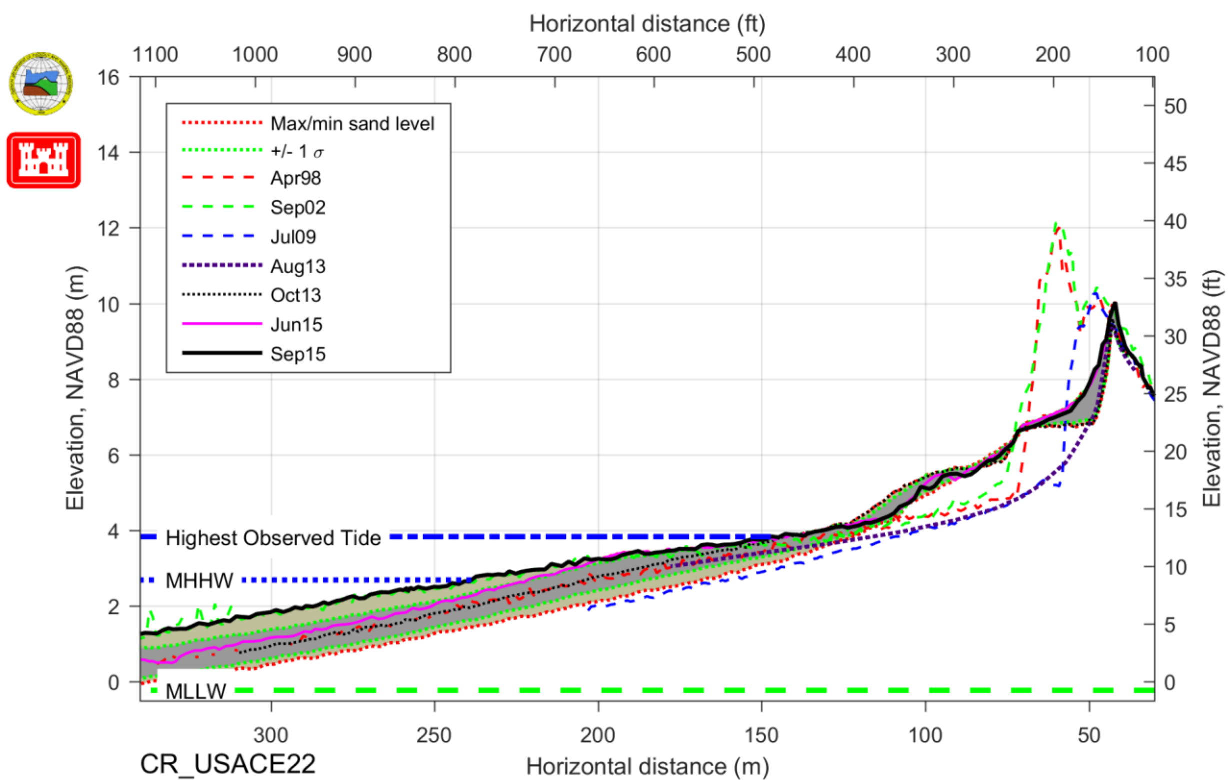
Horizontal distance (ft)
Max/min sand level
+/- 1 σ
Apr98
Sep02
Jul09
Aug13
Oct13
Jun15
Sep15
Highest Observed Tide
MHHW
MLLW
Elevation, NAVD88 (m)
Elevation, NAVD88 (ft)
Horizontal distance (m)
CR_USACE22

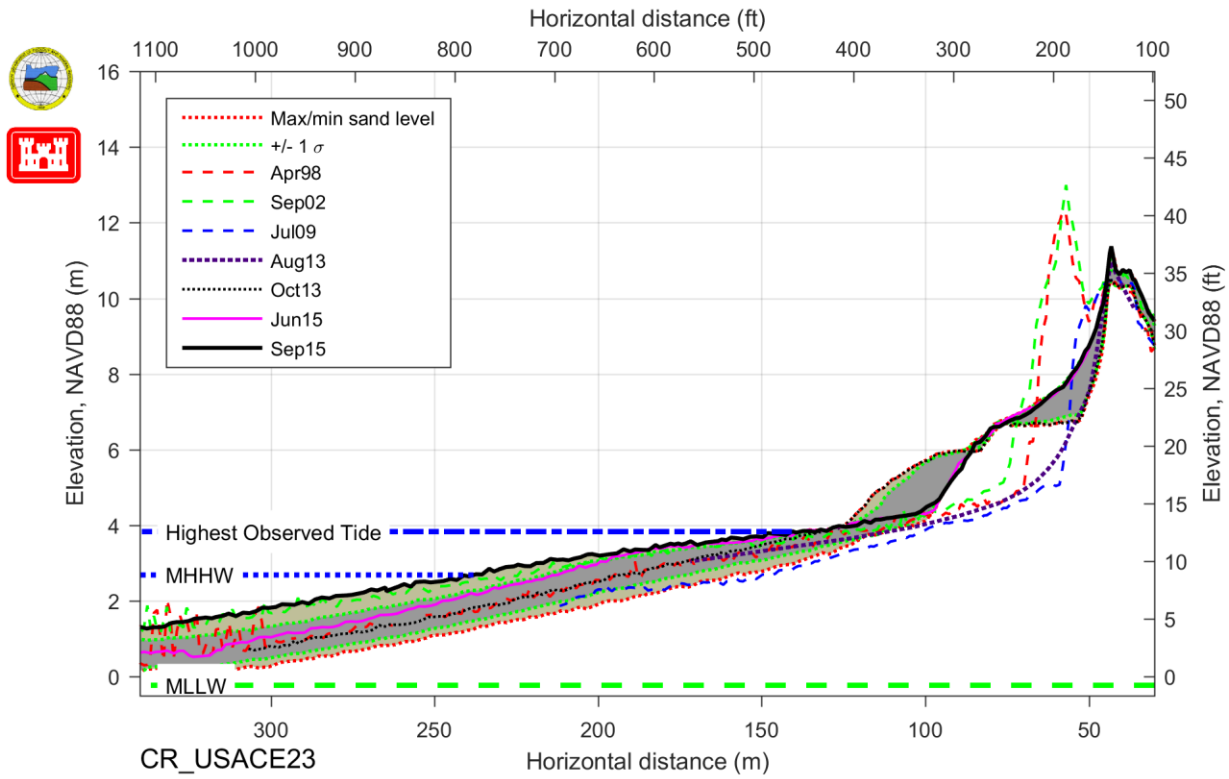
Horizontal distance (ft)
Elevation, NAVD88 (m)
Elevation, NAVD88 (ft)
Max/min sand level
+/- 1 σ
Apr98
Sep02
Jul09
Aug13
Oct13
Jun15
Sep15
Highest Observed Tide
MHHW
MLLW
CR_USACE23
Horizontal distance (m)

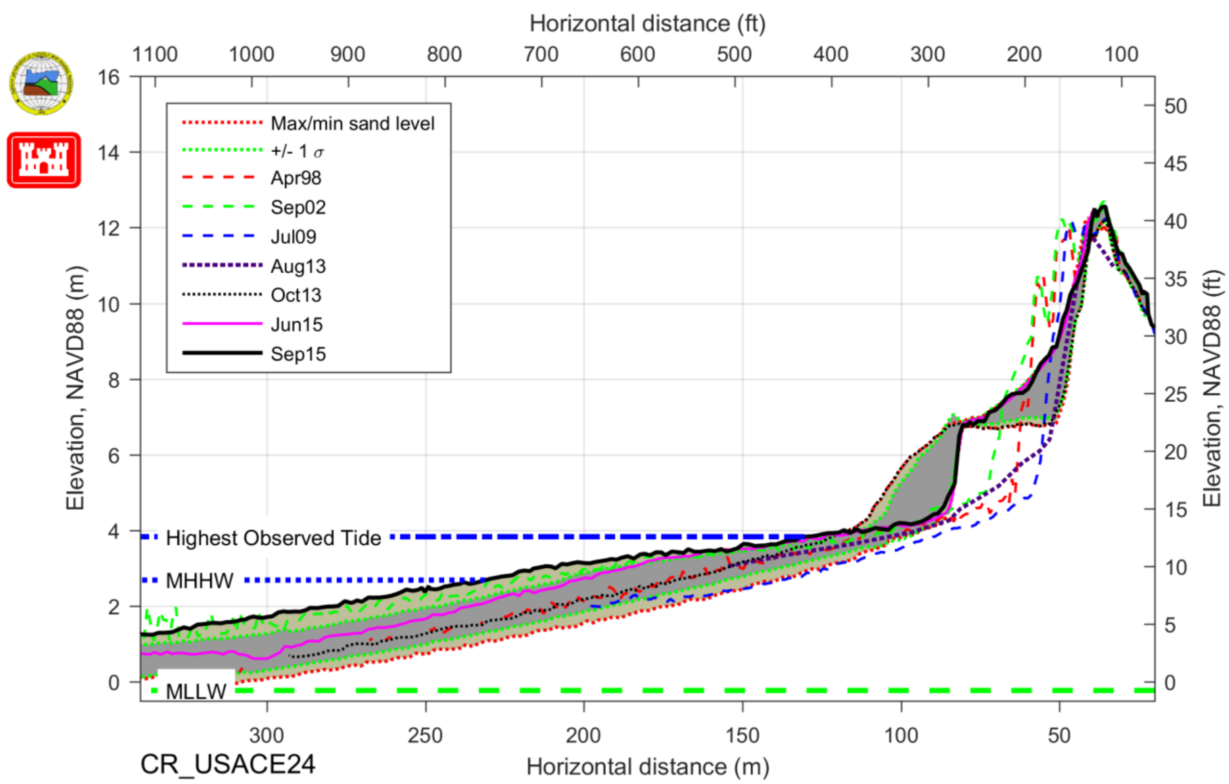
Horizontal distance (ft)
Elevation, NAVD88 (m)
Elevation, NAVD88 (ft)
Max/min sand level
+/- 1 σ
Apr98
Sep02
Jul09
Aug13
Oct13
Jun15
Sep15
Highest Observed Tide
MHHW
MLLW
CR_USACE24
Horizontal distance (m)

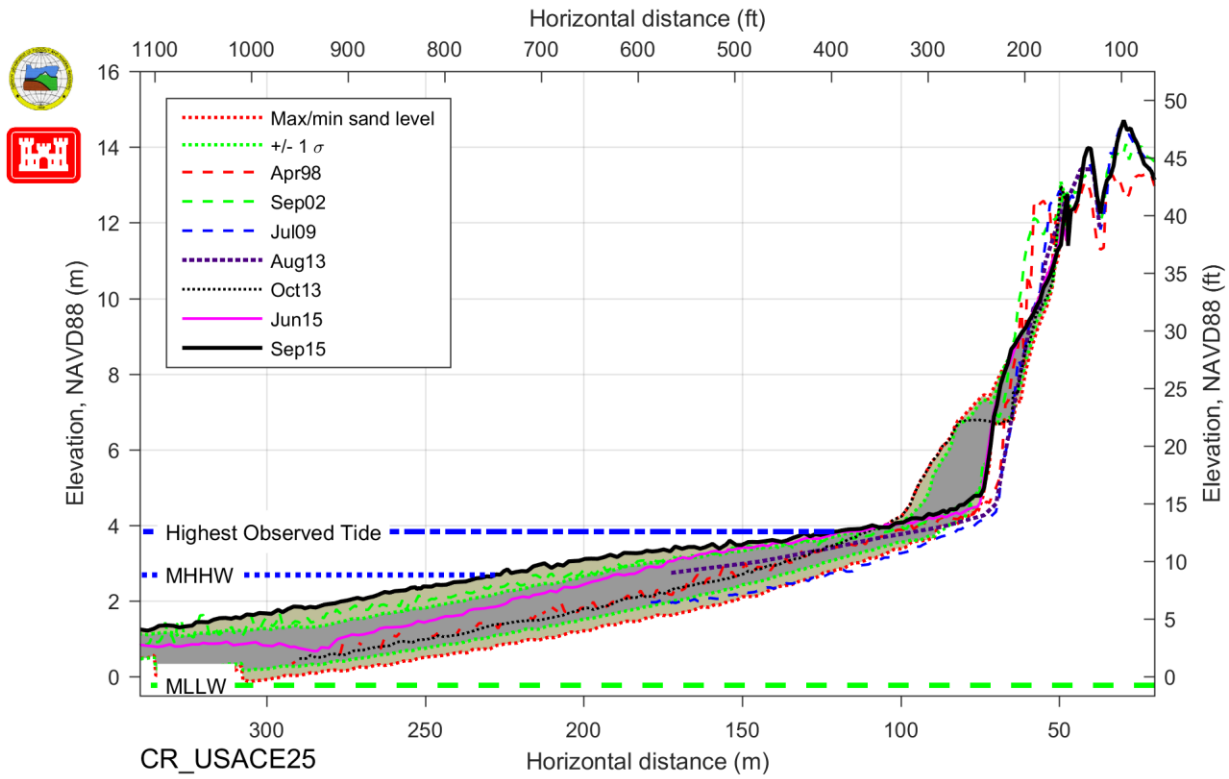
Horizontal distance (ft)
Elevation, NAVD88 (m)
Elevation, NAVD88 (ft)
Max/min sand level
+/- 1 σ
Apr98
Sep02
Jul09
Aug13
Oct13
Jun15
Sep15
Highest Observed Tide
MHHW
MLLW
CR_USACE25
Horizontal distance (m)

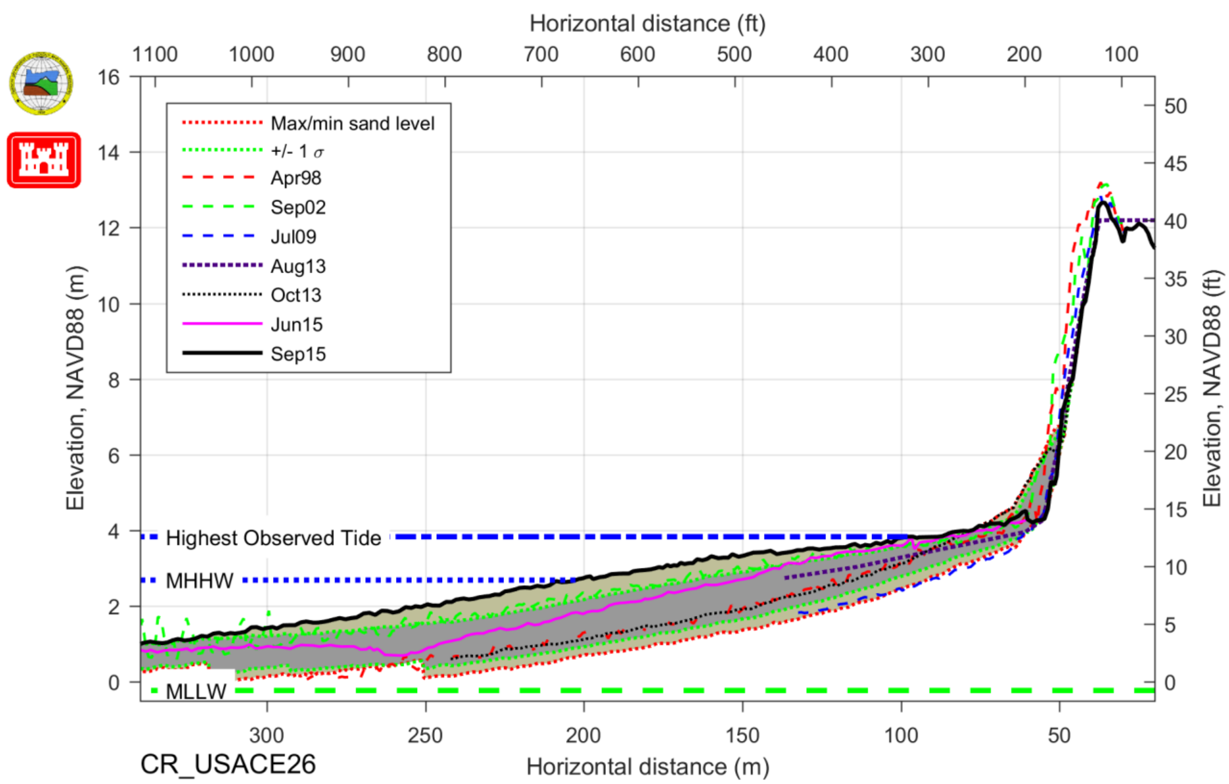
Horizontal distance (ft)
Elevation, NAVD88 (m)
Elevation, NAVD88 (ft)
Max/min sand level
+/- 1 σ
Apr98
Sep02
Jul09
Aug13
Oct13
Jun15
Sep15
Highest Observed Tide
MHHW
MLLW
CR_USACE26
Horizontal distance (m)

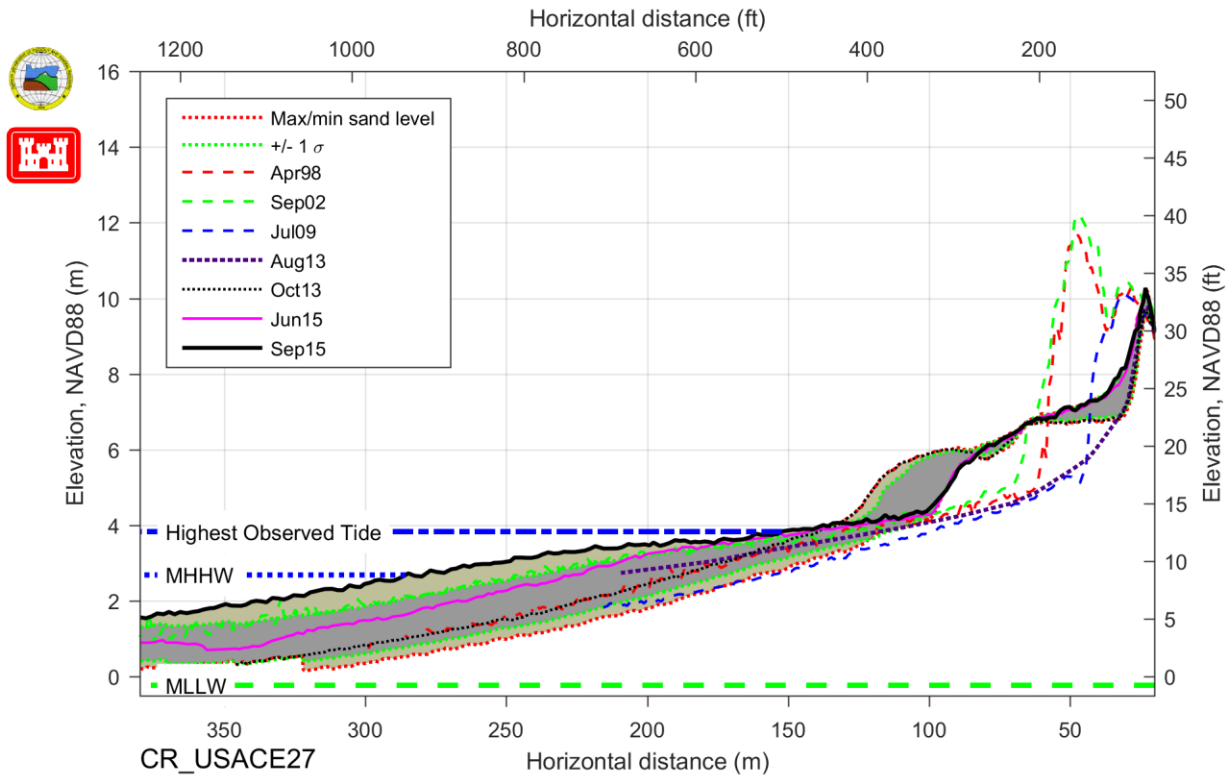

Horizontal distance (ft)
Max/min sand level
+/- 1 σ
Apr98
Sep02
Jul09
Aug13
Oct13
Jun15
Sep15
Highest Observed Tide
MHHW
MLLW
Elevation, NAVD88 (m)
Elevation, NAVD88 (ft)
CR_USACE27
Horizontal distance (m)

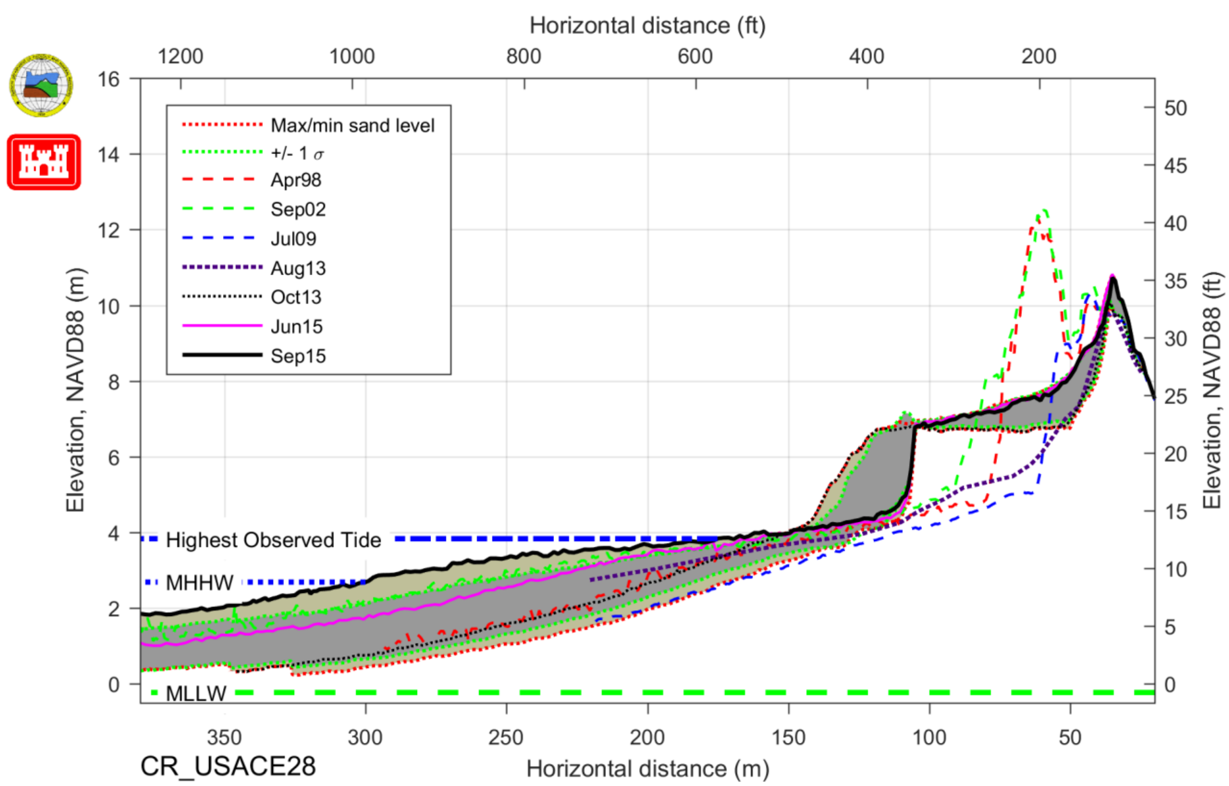

Horizontal distance (ft)
Max/min sand level
+/- 1 σ
Apr98
Sep02
Jul09
Aug13
Oct13
Jun15
Sep15
Highest Observed Tide
MHHW
MLLW
Elevation, NAVD88 (m)
Elevation, NAVD88 (ft)
CR_USACE28
Horizontal distance (m)